RESEARCH DEPARTMENT

A RECONSIDERATION OF LIGHT PATTERN MEASUREMENTS IN LATERAL DISK RECORDING

Report No. C.077
Serial No. 1950/20

Investigation by:

P.E. Axon
W.K.E. Geddes

Report Written by:

P.E. Axon
W.K.E. Geddes

(W. Proctor Wilson)

PRIVATE & CONFIDENTIAL

Research Department July, 1950.

Report No. C.077
Serial No. 1950/20

Figs. No. C.077.1-30
Plates No. C.077.I-VI

A RECONSIDERATION OF LIGHT PATTERN MEASUREMENTS IN LATERAL DISK RECORDING

Summary

The Report describes a new method, which has been developed in the Research Department, of making measurements of the Buchmann-Meyer light pattern of a laterally recorded disk. This pattern is often used to measure the modulation levels of the various frequencies on the disk. The new method is quicker and more simple to use than the traditional method and does not require such a high degree of skill in the operator. The use of the apparatus has revealed the importance of some hitherto unreported optical interference and diffraction phenomena associated with the light patterns. These phenomena are significant in relation to fundamental errors which are inherent in any method of observation of the patterns. The effects are analysed and the Report describes how the simple theory of the light pattern measurement must be modified to give a more accurate result. Part I of the Report describes the new apparatus and the evaluation of the final results of the measurements. Part II contains a detailed analysis and discussion of the various interference and diffraction phenomena which affect the evaluation of the results described in Part I.

PART I

Light Pattern Measurements

1. The Principle of the Light Pattern Method

Figure 1 represents a vertical section through a disk recording inclined to the horizontal so that the outer walls of the grooves at A are vertical and are reflecting light from a distant light source (in the plane of the diagram) back along its incident path. If the grooves be laterally modulated in a sinusoidal manner, the plan view of such a vertical outer wall will be as shown in Figure 2.

A distant observer will see light reflected from all points on the groove where the modulation and the curvature of the groove combine to produce elements perpendicular to the axis. These points will lie out from the central axis only as far as a distance b at which the groove becomes perpendicular to the axis at the point of maximum modulation slope. Beyond this distance there can be no light reflected parallel to the axis. If the disk is rotated, the reflecting points will merge into a band with sharp vertical edges.

When the maximum modulation slope (with respect to an unmodulated groove) is sufficiently small for its sine, tangent and angular measure to be regarded as equal, then the width of the luminous band at any given radius on the disk can be shown to be proportional to this slope, which is in turn proportional to the peak velocity of the recording stylus. Moreover, as the radius of the groove is decreased, the increasing curvature and the increasing slope of the modulation resulting from lower cutting speed exactly counterbalance each other, so that the width of the light band is a function of peak modulation velocity only, independent of radius or frequency.

The assumption that only light parallel to the axis is used in the formation of the light patterns is not justified, however, when light source and viewing aperture are situated at finite distances from the disk, and a formula is derived below which enables the velocity to be deduced from the width of the pattern as measured under practical conditions.

Figure 3(a) represents, in plan, a groove illuminated by a light source of half-width a_2 at a distance d_2 from the disk,

and viewed with a device of aperture half-width a_1 at a distance d_1 from the disk. This arrangement, in which the outer wall of the groove is observed, will henceforward be referred to as the "far-side" method of viewing, as opposed to the "near-side" method, in which the inner wall of the groove is observed, on the side of the disk nearer to the observer. The groove is assumed to have a sinusoidal modulation such that at each point of inflection it is inclined at an angle ϕ with respect to an unmodulated groove (Figure 3b).

Let the half-width of the pattern observed be b_f. Then the extreme right-hand edge of the pattern at P will be formed by light which originates from the extreme left-hand edge of the light source and which enters the extreme left-hand edge of the aperture. The groove is assumed to be oriented so that there is a point of maximum groove slope correctly positioned at P to reflect such extreme rays.

The angles made with the axis by incident and reflected rays are, respectively, $\frac{a_2 + b_f}{d_2}$ and $\frac{a_1 + b_f}{d_1}$ and that made by the normal is their mean:

$$\tfrac{1}{2}\left\{\left(\frac{a_1}{d_1} + \frac{a_2}{d_2}\right) + b_f \cdot \left(\frac{1}{d_1} + \frac{1}{d_2}\right)\right\}$$

The effective radius of curvature of the groove in the plane of the diagram is $R/\cos\theta$, where R is the radius of the groove on the disk, and θ is the angle between the plane of the disk and that of the diagram. The slope between the normal to the groove at P and the axis can also be expressed, therefore, as $\frac{b_f \cos\theta}{R} - \phi$

Equating: $$\phi = \frac{b_f \cos\theta}{R} - \tfrac{1}{2}\left[\left(\frac{a_1}{d_1} + \frac{a_2}{d_2}\right) + b_f\left(\frac{1}{d_1} + \frac{1}{d_2}\right)\right]$$

or $$\frac{R}{\cos\theta}\cdot\phi = b_f\left[1 - \frac{R}{2\cos\theta}\left(\frac{1}{d_1} + \frac{1}{d_2}\right)\right] - \frac{R}{2\cos\theta}\left(\frac{a_1}{d_1} + \frac{a_2}{d_2}\right)$$

If d_1 and d_2 tend to infinity while a_1 and a_2 remain finite, the equation reduces to $\frac{R}{\cos\theta}\cdot\phi = b$, where b is the half-width of the pattern viewed under ideal conditions.

$$\therefore\ b = b_f\left[1 - \frac{R}{2\cos\theta}\left(\frac{1}{d_1} + \frac{1}{d_2}\right)\right] - \frac{R}{2\cos\theta}\left(\frac{a_1}{d_1} + \frac{a_2}{d_2}\right) \quad \ldots\ldots 1(a)$$

Similar reasoning gives, for the half-width observed under "near-side" conditions

$$b = b_n \left[1 + \frac{R}{2\cos\theta}\left(\frac{1}{d_1} + \frac{1}{d_2}\right)\right] - \frac{R}{2\cos\theta}\left(\frac{a_1}{d_1} + \frac{a_2}{d_2}\right) \quad \ldots\ldots\ldots 1(b)$$

The factor multiplying b_n or b_f is henceforward referred to as f_1, (it being understood to apply to Equation 1(a) when less than unity, and to Equation 1(b) when greater than unity), and the term $\frac{R}{2\cos\theta}\left(\frac{a_1}{d_1} + \frac{a_2}{d_2}\right)$ as f_2. When the groove is unmodulated, (i.e. $b = 0$), then Equations 1(a) and 1(b) show that a pattern of width $2f_2/f_1$ is observed, and this residual pattern is henceforward referred to as the "no-mod" band. The equations also show that for any pattern, b_f exceeds b_n by an amount depending on the values of f_1 and f_2. It will now be shown that b is simply related to the modulation velocity, and directly proportional to it.

The angle θ of the optical normal to the disk is equal to half the groove-angle, and Figure 4 shows that the modulation amplitude "m" observed along the optical normal is related to the amplitude M parallel to the disk by the relation $m = M\cos\theta$. As the maximum slope of a sine-wave is proportional to its amplitude, we may replace ϕ by $\Phi\cos\theta$ where Φ is the maximum modulation slope in the plane of the disk

$$\therefore b = \frac{R\phi}{\cos\theta} = R\Phi. \quad \ldots\ldots\ldots 2(a)$$

But $\Phi = \frac{\hat{V}}{2\pi Rn}$ when $\hat{V}$ is the peak stylus velocity and n the revolutions per second of the disk, during recording.

$$\therefore b = \frac{\hat{V}}{2\pi n} \text{ and } V_{R.M.S.} = \sqrt{2\pi nb} \quad \ldots\ldots 2(b)$$

It is desirable that the terms $|1 - f_1|$ and f_2 should be small, so that the accuracy with which the quantities involved in them are known, and the constancy within which they are maintained need not be as high as the overall accuracy required in the experiment. This means that a_1 and a_2 should be kept as small as possible, d_1 and d_2 as large as possible.

Considerations of resolving power and illumination respectively limit the extent to which a_1 and a_2 can be reduced, while d_1 and d_2 increase at the expense of compactness. In the apparatus to be described the constants are as

follows:

$d_1 = d_2 = 48$ inches ($\pm$ 1 inch)

$a_1 = 0.125$ inches

$a_2 = 0.01$ inches

θ is variable, but usually about 47°

These give values for the factor f_1 in Equations 1(a) and 1(b) ranging from about 0.83 and 1.17 at the outside of a 12" disk, to about 0.92 and 1.08 at the inside of the disk. The term f_2 varies from about 0.011 inches to 0.005 inches.

3. New System of Measurement Employed in the Present Apparatus

To blend the individual reflecting elements of a band of tone into a clearly defined pattern, the disk must be rotated, and small deviations from perfect flatness in the disk then cause the pattern to oscillate horizontally. Thus any method of measurement which depends on the alignment of a stationary measuring line to the moving edge of the pattern is both laborious and fatiguing and requires some skill.

In the present apparatus this difficulty is overcome by producing two images of the pattern, movable with respect to each other in a horizontal direction. The width of the pattern is measured by the displacement of the images necessary to cause the left-hand edge of one image to coincide with the right-hand edge of the other image and vice-versa. This alignment is unaffected by oscillation of the pattern, since both images move together in an identical manner. Plate I shows the appearance of the two patterns when adjusted for edge-to-edge coincidence of the 500-cycle bands.

4. Description of Apparatus

4.1 General Layout

The complete apparatus which is shown in Plate II is housed in two angle iron frameworks, each 30" high and 20" wide. In the larger of these, which is 30¼" long, is mounted the disk turntable, while the smaller, 21¼" long, carries the light source and the devices for producing two images and

measuring their separation. The total length of the apparatus is 72½", two further lengths of angle iron holding the frames 20" apart. The apparatus can, of course, be mounted in a single framework of suitable length, but the prototype has been made in two sections so that the disk and measuring devices can be separated for experimental purposes by any desired distance over a certain minimum. The apparatus is self-contained, with the exception of the viewing telescope, which is at present used mounted on a standard tripod. As the telescope is used only as a viewing and not as a measuring device, it is not necessary for it to be rigidly mounted on the framework, although in practice this can be done for greater convenience.

4.2 The Prism System

The twin images are produced by four prisms disposed as in Figure 5. P_1, P_2 and P_3 are mounted on a vertical plate, as are the vertical slits S in front of P_1 and P_3. These slits are ¼ inch wide, compared with the prism width of 1 cm, and so define the aperture $2a_1$ of the system. P_4 is mounted on a turntable rotatable about a vertical axis. The mask M prevents direct observation of the disk through the telescope. When all the prisms are parallel and coplanar the images formed by P_1, P_2 and P_3, P_4, are coincident. When P_4 is rotated about a vertical axis, however, the image formed by P_3 and P_4 is displaced in a horizontal arc, centred on P_4 and of length equal to the optical path from the disk to P_4, and the two images are seen side by side. The moving image also rotates about the line of sight, but as this rotation is only equal in magnitude to the angular displacement of P_4, which is normally less than 1^o, the two images do not become noticeably non-parallel.

The prism system and the mechanism by which the operator can turn P_4 are mounted on a horizontal platform of ½ inch bakelite, 13 inches above the bench. A considerable reduction is required between the operator's control and the rotation of the prism P_4, and this is achieved in two stages. A lead screw (½ inch B.S.F. thread) runs horizontally across the front of the apparatus, and is turned by a handle on the right-hand side of the framework. A threaded block or nut runs on this lead screw and is prevented from rotating by a guide rod. Sprung against the nut, at right angles to its direction of motion, is a horizontal rod which turns a Muirhead slow motion drive. It is on the driven shaft of this that the turntable carrying P_4 rotates. A close-up view

of the prism system and its associated rotational equipment is shown at Plate III.

4.3 The Indicating System

The deflection of P_4 is measured by a reflection method using a concave galvanometer mirror, also mounted on the driven shaft of the slow motion drive, but below the bakelite platform. A lantern, near bench level and between the two frameworks, illuminates the mirror, and the reflected pencil travels to a plane mirror lying across the top of the other framework and thence to a plastic galvanometer scale across the front of the apparatus. The mirror system forms on the scale an enlarged image of a vertical hair line stretched across the front of the lantern.

The scale has a centre zero, and the hair line is arranged to lie at or near this zero when the two images are coincident. Readings are taken on both sides of the coincidence position, and their sum corresponds to twice the total pattern width, provided that both readings are not on the same side of the zero.

This system is calibrated by observations on a graduated scale placed on the turntable, and is found to be linear over the widths encountered. The hair line is read to the nearest $\frac{1}{4}$ millimetre, which corresponds approximately to the nearest thousandth of an inch in the value of b_f or b_n.

A bracket from the main framework holds a ventilated metal box containing a 48 watt lamp which illuminates the disk, shining through a hole sufficiently large to ensure that the entire width of the filament is visible from the disk. The lamp is immediately above the prism system, and the total included vertical angle between incident and reflected light is about 8^o.

4.4 The Turntable Unit

Three factors make it desirable that the turntable carrying the disk should be movable, so that different parts of the disk may be brought to the same point in space for observation.

(1) The effective field of view of the system is less than that of the telescope alone, the extreme bottom of this field being

lost in the image through P_1, P_2, and the extreme top through P_3, P_4. Measurements must only be made, therefore, near the centre of the field.

(2) The factor relating pattern width to angular prism displacement is proportional to the distance from the pattern to the prism P_4.

(3) The depth of focus of the telescope is too small to cover the whole of a stationary disk without re-adjustment.

The turntable assembly is therefore mounted on a wheeled trolley, and two brass rails screwed to diagonals on the sides of the angle iron framework constitute a simple railway inclined at 45° to the horizontal, on which the trolley runs so that the turntable moves parallel to itself. Two Bowden cables run up from the trolley, parallel to the rails, pass over pulleys suspended from the top corners of the framework, and support a lead counterweight. The position of the trolley is controlled by a 1/150th H.P. reversible induction motor, at bench level, to which it is connected over pulleys by two light cables, one for each direction of motion. The motor is operated by a push-button microswitch and a reversing switch, situated near the front of the apparatus adjacent to the observer. As a safety device a microswitch is operated by the trolley at either end of its permissible excursion, and switches off the motor in the outward direction only.

The turntable is rotated by a "Fracmo" motor, geared down to give a speed of about 20 r.p.m. which is just sufficient to merge the luminous elements of a 50 c/s band of tone into a continuous pattern. A slipping clutch protects the gear-box from any torque applied by hand to the turntable.

The yoke carrying the turntable unit is pivoted relative to the trolley about a horizontal axis which allows adjustment of the angle θ between the optical normal of reflection and the disk. This facility is provided to enable θ to be adjusted for a maximum pattern brightness on any disk, the optimum depending on the groove shape. Only when the turntable is parallel to the direction of motion of the trolley, however, is

the distance from the point under observation to the prism system independent of the position of the trolley. This condition is used, therefore, whenever the disk under examination gives a pattern of sufficient brightness, even though this brightness may not be the maximum attainable. For the few disks necessitating adjustment of θ, not only must account be taken of the change in cos θ in Equation 1, but the scale indications must, strictly speaking, be re-calibrated for the extreme positions of the trolley, and b_n and b_f calculated accordingly. The error resulting from neglect of this last consideration is small; if the calibration for say $\theta = 47^o$ is used when θ is in fact 52^o, then the values of b_f and b_n so obtained at the outside of a 12 inch disk will be, respectively, 2% too large and 2% too small.

5. The Accuracy of Buchmann-Meyer Measurements

The measurement of pattern width by the present edge-to-edge method is found to be easy, quick and reproducible within close limits. A disk carrying 16 bands of tone can be examined on both near and far sides in just over half an hour, each setting being performed twice. The accuracy of the system is subject to a limitation which is inherent in the Buchmann-Meyer method, and not peculiar to the present apparatus. As the frequency of the recorded signal is increased, the edge of its associated light pattern becomes less clearly defined, and at frequencies above about 5 kc/s the two images can only be adjusted to merge into each other, rather than to touch. This effect is due to the fact that the law of reflection is only strictly true for reflecting surfaces whose dimensions are very large compared with the wavelength of light, and this condition is not fulfilled by the short reflecting elements occurring in high frequency patterns. As a result, the reflected pencils spread out beyond the limits defined by the law of reflection, and elements reflect into the telescope even when they are some distance outside the calculated edge of the pattern. The effect limits the accuracy of the method at high frequencies to the order of $\pm$ 1 db.

At low frequencies, where the velocities recorded are small, the narrowness of the patterns sets a limit to the accuracy attainable. However the patterns are then sufficiently sharp to yield satisfactory accuracy down to recorded velocities of 15 or 20 db below the standard 1 kc/s r.m.s. velocity of 2 cm/sec.

Apart from the use of disks which have been calibrated with a pick-up of known frequency response, the correctness or otherwise of the results obtained from light pattern measurements can be checked by three methods:

(a) The results obtained from near and far side observations of the same band should be identical.

This is necessarily true for directly recorded disks, where both the inside and the outside of the groove must carry the same modulation, but not necessarily so for pressings, where processing distortion could cause a real difference between the two walls of the groove.

(b) The ratio between two different levels of the same frequency, as measured from their light patterns, should be identical with the ratio of the two voltages applied to the cutterhead provided that it is justifiable to regard the recording process as linear.

(c) Velocity ratios deduced from light pattern measurements can be checked against ratios predicted from measurements of cutterhead voltage under more realistic conditions than those obtaining in (b). Subject to two assumptions set out below, several frequencies can be recorded at known relative velocities, similar to those specified by a typical recording characteristic. The necessary assumptions are firstly that the recording process is linear, and secondly that equality of pattern width between adjacent bands indicates equality of velocity, regardless of frequency. Such an equality of pattern width is first established by trial and error, using a variable attenuator in the recording chain, and the test disk then cut, with the cutterhead voltages modified to give the required recording characteristic.

Of these methods of checking, (a) makes the fewest assumptions, but will not indicate any error which affects near and far side results equally. Methods (b) and (c) are

useful only insofar as they provide clues to the nature of an error indicated by (a) or confirm an indication of correctness given by (a).

6. Typical Results

In the derivation of Equation 1 (Paragraph 2), the edge of the pattern is defined by the extreme position from which a point P, on the surface of the disk, can reflect light into the viewing arrangement. The telescope was accordingly focussed on the surface of the disk for the measurements discussed below. Results are shown in Tables 1, 3 and 5, for three different disks, which will be referred to as disks A, B and C respectively. On disk A, three bands of 1 kc/s tone were recorded at the outside of the disk, and three similar bands at the extreme inside, each set corresponding to relative applied voltages of 0, -10 db and -20 db respectively.

Disk B is of the type described in 5(c) above. As in disk A, two similar sets of bands were recorded, one at the outside and one at the inside of the disk, each set containing bands at 1, 0.5, 0.2 and 0.1 kc/s, and a further band of 0.1 kc/s tone suitably attenuated to simulate the normal recorded level of 0.05 kc/s.

Disk C is a Multifrequency Test Record (B.B.C. Reference No. DOM 46) covering the range 10 kc/s to 0.05 kc/s, recorded with the T.R.U. recording characteristic. A careful pick-up calibration of this disk has previously been carried out by Designs Department.

It will be seen that, with the exception of the inside set of bands on disk A, the value of the ideal pattern half-width, b, (Equations 1 and 2) is in every case greater when deduced from b_f than when deduced from b_n. When low velocities are recorded near the outside of the disk, the discrepancy becomes very large, exceeding 4 db for the band of lowest velocity on disk A, and 2 db for that of disk B. The extreme velocity ratios deduced from far side measurements are found to be slightly greater than those predicted from voltage considerations, and those deduced from near side measurements, considerably greater.

The systematic error exhibited in these results is attributed to the fact that no account has so far been taken of effects due to the wave properties of light, and these will now be considered.

7. Influence of the Wave Properties of Light

The system has so far been assumed to obey precisely the laws of geometrical optics; no account has been taken of diffraction or interference effects. Two phenomena have been observed, however, which can only be explained in terms of diffraction and interference theory. The first phenomenon is a black line running down the centre of the "no-mod" band under certain viewing conditions, whilst the second is the occurrence of brightly coloured vertical striations across high frequency patterns. These phenomena are discussed in detail in Paragraphs 8 and 9.

In Paragraph 8 the conclusion is reached that the "no-mod" band actually observed is narrower than that calculated geometrically. Moreover, at low frequencies and long wavelengths it seems reasonable to assume that the curvature of a groove near its point of maximum slope will be very nearly that of the unmodulated groove, so that the elements forming the edge of the pattern will reflect in a similar manner to those forming the "no-mod" band, and will for the same reasons be observed narrower than the calculated geometrical values. Although this argument cannot be extended to cover higher frequencies, it is clearly desirable to consider any alternative method of observation which would not be susceptible to this error. Such a method is suggested by the investigation of the coloured interference fringes, described in Paragraph 9. These fringes are found to be localised in a plane which also contains the image of the light source formed by the unmodulated grooves. When the telescope is focussed on this "focal plane", a sharp-edge light pattern is seen, even though the surface of the disk is out of focus. It is demonstrated in Paragraph 10 that in fact the width of this sharp edge pattern observed in the focal plane is the same as would be derived from purely geometrical constructions. A fresh series of observations has therefore been made with the telescope focussed on this "focal plane".

A simple geometrically derived formula (Paragraph 11) enables the half-widths measured on the focal plane, to be converted to hypothetical values of b_f and b_n respectively, and hence to values of b, using Equations 1(a) and 1(b).

When the telescope is focussed on the disk, complex diffraction effects are believed to occur, and it is doubtful whether normal considerations of resolving power are relevant. If the resolving power is in fact calculated and a correction made for it, the result is to increase the discrepancy between

the observed and predicted velocity ratios, and also to increase, slightly, the near to far error. Observations on the focal plane of the disk are, however, carried out on the assumption that the resolving power of the system is then the only relevant aspect of diffraction remaining and hence a correction is made for it in the evaluation of results. In paragraph 12 an expression is derived for the resolving power of a telescope when used to view an object at a finite distance from its objective.

Taking the average wavelength of white light as 2×10^{-5} inches, a_1 as 0.125 inches and d_1 as 48 inches, the present system is seen to be incapable of resolving points closer than 0.004 inches. This means that the two images of a pattern will appear to touch when they are 0.004 inches apart, so that the observed value of the half-width will be too large by 0.002 inches. If a correction is made for this so that the measurement may be assumed to give a width reliable to 0.001 inches, then the result will be liable to an uncertainty of about $\pm$ 0.5 db for the narrowest bands normally encountered, and proportionately less for wider bands. This resolving power gives a picture which appears satisfactory to the eye although the resolution is not as high as that which the eye would achieve for a perfect image, at the magnification employed.

To increase the resolving power of the system, while maintaining the present distance between the disk and prisms, would necessitate the use of larger and more expensive prisms and consequently of a telescope with a larger objective. It therefore seems preferable to correct for the present resolving power, as outlined above, and to keep the cost of apparatus low.

8. Results Obtained from "Focal Plane" Observations

The measurements made on disks A, B and C with the telescope focussed to give the narrowest possible "no-mod" band, give the results shown in Tables 2, 4 and 6 respectively.

It will be seen that there is still a tendency for higher values of b to result from far side than from near side observation, but that the difference seldom exceeds 0.5 db, and shows no tendency to increase at low levels. Thus the velocity ratios deduced from b_f'' show good agreement with those deduced from b_n'', and moreover these ratios agree closely with those predicted by voltage measurements or, in the case of disk C, with the pick-up calibration.

TABLE 1

Disk A - Telescope focussed on disk surface

Radius of Band in Inches	Freq. of Band in kc/s	b (from b_f) thousandths of an inch	b (from b_n) thousandths of an inch	Ratios - far (db)	Ratios - near (db)	b (from b_f) / b (from b_n) (db)	Ratios (from Voltage) (db)
5.5	1	148	144½	0	0	+0.2	0
5.3	1	43	39½	-10.7	-11.3	+0.7	-10.0
5.0	1	11½	7	-22.2	-26.3	+4.3	-20.0
2.6	1	146½	147½	0	0	-0.1	0
2.5	1	43½	44	-10.6	-10.5	-0.1	-10.0
2.3	1	12	12	-21.7	-21.8	0	-20.0

Notes: 'b (from b_f)' and 'b (from b_n)' - half widths of ideal pattern (see Equations 1 and 2) calculated from far side and near side observations respectively.

TABLE 2

Disk A - Telescope focussed on 'Focal Plane' of disk

Radius of Band in Inches	Freq. of Band in Kc/s	b (from b_f) thousandths of an inch	b (from b_n) thousandths of an inch	Ratios - far (db)	Ratios - near (db)	b (from b_f) / b (from b_n) (db)	Ratios (from Voltage) (db)
5.5	1	149½	152	0	0	-0.2	0
5.3	1	46½	47	-10.1	-10.2	-0.1	-10.0
5.0	1	13½	13½	-20.9	-21.0	0	-20.0
2.6	1	148½	152½	0	0	-0.2	0
2.5	1	46	46½	-10.2	-10.3	-0.1	-10.0
2.3	1	13½	14	-20.8	-20.7	-0.3	-20.0

Notes: (Cont.) 'Ratios-far' and 'Ratios-near' - the columns 'b (from b_f)' and 'b (from b_n)' respectively, expressed as ratios, relative to the value of b underlined, for each set of bands.

$\frac{\text{'b (from } b_f\text{)'}}{\text{'b (from } b_n\text{)'}}$ - comparison between the two levels deduced for each band.

TABLE 3

Disk B - Telescope focussed on disk surface

Radius of Band in Inches	Freq. of Band kc/s	b (from b_f) thousandths of an inch	b (from b_n) thousandths of an inch	Ratios - far (db)	Ratios - near (db)	b (from b_f) / b (from b_n) (db)	Ratios (from Voltage) (db)
5.5	1	118½	110½	0	0	+0.6	0
5.3	0.5	97	89	-1.7	-1.9	+0.8	-1.7
5.1	0.2	66½	59½	-5.0	-5.4	+1.0	-4.7
4.9	0.1	47	40	-8.0	-8.8	+1.4	-8.1
4.7	0.1	23½	18½	-14.0	-15.5	+2.1	-13.6
3.4	1	119	114	0	0	+0.4	0
3.2	0.5	97	91½	-1.8	-1.9	+0.5	-1.7
3.0	0.2	67½	64	-4.9	-5.0	+0.5	-4.7
2.9	0.1	48	44	-7.9	-8.3	+0.8	-8.1
2.6	0.1	24½	22½	-13.7	-14.1	+0.7	-13.6

TABLE 4

Disk B - Telescope focussed on 'focal plane' of disk

Radius of Band in Inches	Freq. of Band kc/s	b (from b_f) thousandths of an inch	b (from b_n) thousandths of an inch	Ratios - far (db)	Ratios - near (db)	b (from b_f) / b (from b_n) (db)	Ratios (from Voltage) (db)
5.5	1	122½	118½	0	0	+0.3	0
5.3	0.5	99	96	-1.8	-1.8	+0.3	-1.7
5.1	0.2	69	67	-5.0	-5.0	+0.3	-4.7
4.9	0.1	48	46½	-8.1	-8.1	+0.3	-8.1
4.7	0.1	25	24½	-13.8	-13.7	+0.2	-13.6
3.4	1	122	119	0	0	+0.2	0
3.2	0.5	99	96½	-1.8	-1.8	+0.2	-1.7
3.0	0.2	69	67½	-4.9	-4.9	+0.2	-4.7
2.9	0.1	48½	46½	-8.0	-8.2	+0.4	-8.1
2.6	0.1	25½	24½	-13.6	-13.8	+0.3	-13.6

TABLE 5

Disk C - Telescope focussed on disk surface

Radius of Band in Inches	Freq. of Band kc/s	b (from b_f) thousandths of an inch	b (from b_n) thousandths of an inch	Ratios - far (db)	Ratios - near (db)	b (from b_f) / b (from b_n) (db)	Ratios from Pick-up Calibration
5.5	1	157½	140½	+0.1	-0.2	+1.0	0
5.3	10	156½	143	0	0	+0.8	0
5.1	9	158	142½	+0.2	-0.1	+0.9	0
4.9	8	158	144	+0.2	0	+0.8	0
4.7	7	162½	142½	+0.4	-0.1	+1.1	0
4.5	6	157	140½	+0.1	-0.2	+1.0	0
4.3	5	154	141½	-0.1	-0.1	+0.7	0
4.2	4	154½	142	-0.1	-0.1	+0.7	0
4.0	3	152	142½	-0.1	-0.1	+0.6	0
3.8	2	155	143½	0	0	+0.7	0
3.6	1	155½	143½	0	0	+0.7	0
3.4	0.5	139	127½	-1.0	-1.0	+0.7	-1.0
3.2	0.2	91½	83	-4.6	-4.7	+0.8	-4.5
3.0	0.1	46½	39	-10.5	-11.3	+1.5	-10.5
2.8	0.05	21	17	-17.4	-18.5	+1.8	-17.5
2.6	1	162½	153½	+0.4	+0.6	+0.5	0

TABLE 6

Disk C - Telescope focussed on 'focal plane' of disk

Radius of Band in Inches	Freq. of Band kc/s	b (from b_f) thousandths of an inch	b (from b_n) thousandths of an inch	Ratios - far (db)	Ratios - near (db)	b (from b_f) / b (from b_n) (db)	Ratios from Pick-up Calibration
5.5	1	162½	147½	+0.3	0	+0.8	0
5.3	10	157	149	0	+0.1	+0.4	0
5.1	9	156½	146	0	0	+0.6	0
4.9	8	152½	147	-0.2	0	+0.3	0
4.7	7	154½	147½	-0.1	0	+0.4	0
4.5	6	153½	145	-0.2	-0.1	+0.5	0
4.3	5	153½	144½	-0.2	-0.2	+0.5	0
4.2	4	153	147½	-0.1	0	+0.3	0
4.0	3	154½	147½	0	0	+0.4	0
3.8	2	156½	148½	0	+0.1	+0.4	0
3.6	1	156½	147	0	0	+0.5	0
3.4	0.5	140½	131½	-0.9	-1.0	+0.6	-1.0
3.2	0.2	91½	87½	-4.7	-4.5	+0.4	-4.5
3.0	0.1	46½	43½	-10.5	-10.6	+0.6	-10.5
2.8	0.05	21	21	-17.4	-16.9	0	-17.5
2.6	1	163½	156	+0.4	+0.5	+0.4	0

PART II

Special Optical Conditions in the Light Pattern Formation

8. The Black Line in The Centre of the "No-mod" Band

8.1 When the "no-mod" band is viewed in the far side position, and at the outside of a 12 inch disk, a black line is observed running down its centre. A photograph of part of the light pattern of a disk in which this black line is evident is shown at Plate IV. Nearer the inside of the disk, or in the near side position, the line can also be observed, but only by altering slightly the focus of the telescope.

8.2 Explanation of the Phenomenon

When the telescope is focussed on any point D on the disk surface (Figure 6) the length of the optical path from D to its image is the same for all rays. Now suppose a constant length is subtracted from all these rays by drawing an arc R_d centred on D. The path length from this arc to the image will be constant for all rays, so that the vector summation of all disturbances taken on this arc will give the same illumination as that observed at the image of D. The reflected rays forming the image, however, come to a focus at F, the image of the light source formed by the disk, and are thus in phase at F and along any arc centred on it, such as R_f.

The two arcs R_d and R_f can be made to touch at a point on the line DF produced; if D lies within the width of the "no-mod" band, this line will pass through the viewing aperture, and the radii of R_d and R_f can be chosen so that the two arcs touch at some point O in the aperture.

The disturbance reaching R_d at any point P along its length will have a phase angle $(-2\pi\ \delta/\lambda)$, relative to the disturbance at the point O, δ being the separation of the two arcs at P. If, therefore, the arc R_d be divided into a large number of elements, each of a length L over which a mean value of δ is taken, the light reaching each of these elements may be represented by a vector of constant length proportional to L, oriented according to the mean value of the phase angle $(-2\pi\ \delta/\lambda)$. The illumination observed at D, which is the vector sum of all the disturbances along R_d, will be determined by the resultant of these vectors (Figure 7a). The intensity of illumination will actually be proportional to the square of the resultant vector, which represents amplitude. If the length L is now made vanishingly small, the vector diagram becomes a continuous curve, (Figure 7b), equal lengths along the curve representing equal lengths

along the arc R_d. To find the shape of this curve, it is necessary to determine the variation of δ across the aperture.

Consider the respective separations q_1 and q_2 of the arcs R_d and R_f from their common tangent, at a distance e from their point of contact O, (Figure 8). If the radii of the two arcs are r_d and r_f, it can be shown that $q_1 = \frac{e^2}{2r_d}$ and $q_2 = \frac{e^2}{2r_f}$.

The path difference δ should properly be taken along a radius of the arc R_f. With the dimensions actually involved (as opposed to those adopted for convenience in the Figure) this radius is very nearly perpendicular to the common tangent, since $e \ll r_f$, and so δ may be taken as equal to $q_2 - q_1$.

$$\therefore \delta = \frac{e^2}{2}\left(\frac{1}{r_f} - \frac{1}{r_d}\right) \quad \ldots\ldots\ldots\ldots(3)$$

The variation of the effective path difference δ across the aperture is thus seen to be proportional to the square of the distance from the point O, for which δ is zero.

Such a square-law relationship is often encountered in the consideration of cylindrical wave-fronts, and the generalised vector diagram has a standard form known as "Cornu's Spiral" (Figure 9). This is derived from the Fresnel integral, used in classic diffraction theory. Only that part of the spiral corresponding to values of δ from zero to 3λ is shown, the remainder of the curve (corresponding to higher values of δ) converging on the asymptotic points at J and J. Any length along the arc R_d in either direction from the point of contact with R_f is represented in the vector diagram by an equivalent length along the spiral in either direction from the point of inflection, and it is now necessary to find the value of this equivalence, i.e., the length of the spiral which represents the length $2a_1$ of the arc R_d. This is done by finding the value of δ at the edges of the aperture when D is in the centre of the "no-mod" band and the arcs R_d and R_f touch at the centre of the aperture. The following values are substituted in Equation 3.

$e = a_1 = 0.125$ inches

$r_d = 48$ inches

$r_f = 43.5$ inches (F is 4.5 inches in front of the disk when the outside of a 12 inch disk is viewed in the far-side position)

δ is found to be 1.7×10^{-5} inches, or approximately $7/8\lambda$, at each edge of the aperture. Thus when D is in the centre of the "no-mod" band, the portion of the spiral representing the disturbances along R_d is as shown by the curve AA' (Figure 10), and the intensity observed at D is proportional to the square of the chord AA'. The length of the arc R_d is always $2a_1$, regardless of where it touches the arc R_f, and the derivation of the Cornu spiral is such that in this case the length of the curve AA' representing the disturbances along the arc is also constant. The position of AA' on the spiral will, however, depend on the position of the point of contact of the arcs R_d and R_f, with respect to the aperture. When, for example, the edge of the "no-mod" band is viewed, the two arcs touch at the edge of the aperture, and so one end of the curve AA' lies at the point of inflection (Figure 11). Changes in the position of D may therefore be imagined as causing the constant length of the curve AA' to slide along the spiral.

If the intensity of illumination, which is proportional to the square of the chord AA', is investigated as D is moved from the centre of the "no-mod" band to its edge and beyond, it is found first to increase (Figure 12) and then to decrease again, until at the edge of the pattern (as in Figure 11) it is considerably less than at the centre. As D is moved still further in this direction, the arcs R_d and R_f no longer touch at any point on the aperture, AA' is entirely to one side of the point of inflection and the resultant steadily decreases (Figure 13). It can also be seen that the length of AA' when D is at the centre of the "no-mod" band is a minimum which accounts for the observation of a dark line there. Now the intensity at the edge of the pattern is less again than that of the central minimum, so that the "no-mod" band will be observed as being somewhat narrower than its geometrically calculated width. It will be seen that when the length of the curve AA' is slightly less than that considered here, the centre of the band will no longer be at a minimum of illumination. This accounts for the fact that the central black line is not observed on the near-side of the disk, nor at small disk radii on the far-side, under which conditions the maximum value of δ is smaller than calculated above, unless increased by alteration of the telescope focus. The illumination, however, will still fall considerably below its maximum value as the edge of the pattern is approached, so that the reduction of the observed width of the "no-mod" band below its calculated value will occur under all normal observation conditions.

9. The Formation of Interference Fringes on the Light Patterns

9.1 Appearance of the Fringes

When the light patterns on a multi-frequency tone disk are examined, either through a telescope or with the naked eye, radial striations or fringes are observed across the patterns for frequencies above about 0.5 kc/s. A typical pattern containing the fringes is shown at Plate V. The fringes are found to be located not on the surface of the disk, but upon the plane in which the grooves form an image of the light source. This plane, which lies behind the convex groove surface observed in the near-side position and in front of the concave surface observed in the far-side position, will henceforward be referred to as the "focal plane" of the disk.

At high frequencies the fringes near the edge of the pattern are broad, widely spaced and appear almost black whilst nearer the centre of the pattern their appearance changes and they become narrower, closer together and coloured. The first black fringe is always an appreciable distance from the edge of the pattern. When lower frequencies are observed the fringes begin nearer to the edge of the patterns, and are everywhere narrower and closer together. At frequencies between about 2 kc/s and 0.5 kc/s (on a normally arranged tone disk) only the first few (outside) fringes can be seen, their intensity decreasing towards the centre of the pattern. When the disk is viewed in the conventional manner for measurements of pattern width, that is with the telescope focussed on the surface of the disk, the fringes are still distinguishable on the high frequency bands but are less distinct than when the telescope is focussed on the focal plane of the disk. The following paragraphs will show that the interference pattern observed is formed by the combination of two distinct system of fringes. The first of these systems, described in paragraph 9.2, is caused by the path difference between the two pencils of light which are reflected in a given direction from each wavelength of modulation. Thus in Figure 14 the pencil K' is seen to correspond to a longer total path from light source to image than that in the case of the pencil K. As the path difference is governed by the amplitude m of the modulation, these fringes will be referred to as "m" fringes. The second system, described in Paragraph 9.3, is due to the path difference at a point in the focal plane between pencils reflected from successive cycles of modulation (Figure 15). In this case the path difference

is a function of the wavelength W of the modulation along the groove, and not of its amplitude, and the fringes will be referred to as "W" fringes.

9.2 The Mechanism of the Formation of "m" Fringes

Consider a cylindrical mirror forming an image P_o of a distant object on a plane at distance p from the mirror. Then if a short length of the mirror is divided into a number of strips parallel to the axis of the cylinder, and if these strips are all rotated through a small angle γ (Figure 16), the image formed by each of the strips will move to the position P_γ, where $P_oP_\gamma = 2\gamma P$. The image is, therefore, displaced but not destroyed by this process. If now this slatted cylindrical mirror is replaced by a modulated groove of the same curvature, then the plane at distance p becomes the focal plane of the disk, and the point P_o the image of the light source formed by the unmodulated groove. Figure 17 shows that when a point P_γ in the focal plane is viewed through an aperture AA', only light which is reflected from a small region XX' on the groove is accepted. The extent of XX' is approximately equal to YY', which is the width calculated for the "no-mod" band when a point source of light is used (i.e. $a_2 = 0$). The illumination at a point P_γ in the focal plane, due to light reflected from one wavelength of the modulation, situated within the region XX', can be found by the construction in Figure 18.

The arcs R and R' are hypothetical sections of the unmodulated groove, turned through an angle γ, and they touch the modulated groove at B and B' respectively, these being the points of modulation slope γ, which lie to either side of a point S of maximum modulation slope. Now if the arc R were a reflecting surface, it would form a focus at P_γ, as shown above and so disturbances reflected from all points on the arc would arrive at P_γ in phase. The disturbances from any points on the actual groove around B will therefore arrive at P_γ with relative phases depending on the separation of their points of reflection from R. Reflection from a point for which this separation is δ, involves and optical path which exceeds that of disturbances reflected from B by a distance 2δ, since the incident light has also to traverse an additional distance δ before reaching the reflecting surface. The distance δ increases with distance along the groove from B, slowly at first and then rapidly, so that without investigation of the mathematical form of the variation, it can be seen that the vector diagram will be a spiral of some description converging,

for elements remote from B, towards asymptotic points. As the displacement towards B' is continued, however, the rate of increase of δ reaches a maximum at the point S, and then decreases again, so that the vector diagram begins to spiral outwards again and then describes a figure corresponding to the variation of δ around B' (Figure 19). It is more convenient, therefore, to sum the region around B only as far as the point S in the direction of B', and then to construct a separate vector diagram for reflection from the region around B', only including points towards B as far as S (Figures 20a and b). The respective resultant of these two diagrams will have the same phases as the disturbances reflected from some points C and C' near B and B'.

The illumination observed at P_γ due to reflection from the groove over this wavelength of modulation is therefore a maximum or a minimum according to whether the path length from light source to P_γ via C' exceeds that via C by an odd or even number of half wavelengths of light. Moreover, the situation of the arcs R and R' with respect to the modulation is a function of γ only, and does not depend on the position along the groove of the wavelength of modulation considered. Consequently, conditions for a maximum, or a minimum, at P_γ are satisfied simultaneously by all those wavelengths of modulation which are correctly positioned to reflect light into the viewing aperture through P_γ (i.e. those which lie within the region XX' in Figure 17).

As γ decreases the points B and B' move away from the point S, until for $\gamma = 0$ they are at the points of zero modulation slope and maximum modulation displacement. The path differences involved, therefore, increase with decrease of γ, slowly at first and then more rapidly, thus accounting for the observed decrease in the spacing of the fringes towards the centre of the pattern. As the wavelength of the modulation is increased, a stage is reached at which the two interfering portions of each wavelength are within a distance XX' (Figure 17) of each other only for large values of γ. As a result, only the first few fringes are realised, and this is in fact the condition observed for frequencies around 1 kc/s. At still lower frequencies the physical separation of the interfering portions exceeds XX' before γ is sufficiently small to give the first minimum, and the fringes disappear altogether.

The above account, then, describes the mechanism which determines the amount of light reflected from any one cycle of modulation in the direction defined by the point P_γ. When the

wavelength of the modulation is sufficiently small for two or more cycles to lie within the region XX', the possibility occurs of interference between contributions from the individual cycles, and the resulting system of fringes is described below.

9.3 The Mechanism of the Formation of "W" Fringes

The previous paragraph has demonstrated that the resultant light reflected from each half cycle of groove modulation has the same phase as a single ray reflected from some equivalent point (C or C' in Figure 21) which lies with the half cycle. It is convenient now to compound the two equivalent rays from C and C' of each cycle into a single resultant which in turn may be represented in phase by a ray reflected from some new equivalent point. For each cycle of modulation there is then an equivalent point and the equivalent points of all adjacent cycles will be separated by a distance equal to the modulation wavelength W. Consider, therefore, an unmodulated groove whose surface absorbs light completely except for infinitesimal elements spaced along it at intervals of length W, which scatter light uniformly in all directions. Let two successive scattering elements Z_1 and Z_2 each be joined to P_o and P_γ, where P_o and P_γ are defined as before, so that angle $P_oZ_1P_\gamma$ and angle $P_oZ_2P_\gamma$ are both equal to 2γ (Figure 21). Let an arc centred on P_o and passing through Z_2 cut Z_1P_o at T, and let an arc centred on P_γ and passing through Z_1 cut Z_2P_γ at U. Since P_o is an image point the difference Z_1T between the reflected paths Z_1P_o and Z_2P_o must be equal and opposite to the difference in the respective incident paths from the light source to Z_1 and Z_2. The reflected path difference Z_2U between Z_1P_γ and Z_2P_γ together with the incident path difference (equal to Z_1T) then gives a total path difference to P_γ of (Z_2U+Z_1T). The two arcs intersect at an angle 2γ, so that

$$(Z_2U + Z_1T) = 2\gamma W = G$$

where G is the path difference for light reaching P_γ from successive elements.

Thus for a groove modulated with a signal of wavelength W, G is the path difference between the resultant pencils reflected from successive wavelengths of modulation. The illumination at P_γ is a maximum whenever G is equal to $n\lambda$, where the integer n defines the 'order' of the fringes of n. If there are N wavelengths of modulation simultaneously operative, then the illumination falls to zero for a change

of λ/N in the value of G. This is illustrated for N = 6 in Figure 22. The maxima thus become narrower for large values of N (i.e. at high frequencies).

9.4 Combination of "m" and "W" Fringes

The "m" fringes may be considered as 'modulating' the "W" fringes, since only such illumination as reaches P_γ from the individual wavelengths is available to form the corresponding "W" fringe. When a 10 kc/s signal is recorded at an r.m.s. velocity of 4 cm/sec (line-up level for the B.B.C. recording characteristic at 10 kc/s), at a radius of 5½ inches, then $W = 4.5 \times 10^{-3}$ inches and the maximum slope of modulation ϕ equals 0.05 radians, so that at the edge of the pattern ($\gamma = \phi$) the quantity G is equal to 4.5×10^{-4} inches, corresponding to "W" fringes of about the 20th order. Consequently the overlapping of the fringes due to the different wavelengths present in white light is sufficient to cause the illumination to be observed as uniform. Near the centre of the pattern, however, the "W" fringes are of low order, and it is these fringes which are observed rather than the high order "m" fringes.

If the recorded level of high frequency tone is lower, however, the first minimum of the "m" fringes occurs nearer to the centre of the pattern, whereas the "W" fringes are unaffected, and so are still of a sufficiently low order to be visible outside the first black "m" fringe. Since these "W" fringes are observed as a variation of colour rather than of intensity it is not easy to photograph them in monochrome. They are not evident in Plate V although the directly observed pattern on the disk showed them quite plainly. For still lower levels, which are fortunately lower than those likely to be encountered on a tone disk, the "W" fringes are still strongly visible at the edge of the pattern, thus making the measurement of its width difficult. The "W" fringes can be demonstrated very clearly by increasing the angle θ between the optical normal and the disk surface. This causes the component of the modulation amplitude parallel to the normal to be reduced so that the condition for the formation of the first black "m" fringe is fulfilled at a point on the focal plane nearer the centre of the pattern. At the same time the spacing of the "W" fringes is increased and their order at the edge of the pattern thereby lowered giving an increase of intensity and contrast. It is then possible to photograph them. In Plate VI which was taken under these conditions, the uniformly spaced "W" fringes can be seen clearly outside the first black "m" fringe.

10. Validity of Observations on the Focal Plane

Application of the construction of Figure 18 to the case where γ is equal to ϕ, the maximum slope of the modulation, shows that at low frequencies the light pattern observed has a sharp edge at the position on the focal plane predicted by geometrical considerations, so that measurements can be carried out with the telescope focussed on this plane. In Figure 23 the illumination at Pϕ due to light reflected from one wavelength of modulation is found by summation along an arc R, which is a hypothetical section of the unmodulated groove turned through an angle ϕ. The arc touches the modulated groove at S, the point of maximum modulation slope, and it is in this case convenient to construct a single vector diagram for the summation of disturbances reflected from the groove around S.

As a sine wave is very nearly linear near its point of inflection, the modulated groove near S is of almost the same curvature as the unmodulated groove, and so is nearly coincident with R. For points further from S the separation δ of the groove from R increases rapidly, and the vector diagram is therefore of the approximate form shown in Figure 24(a). Its curvature is in the same sense throughout, since δ is positive to one side of S and negative to the other. If now a point on the focal plane is examined for which γ exceeds ϕ by a very small angle μ, and arc centred on $P_{(\phi+\mu)}$ cuts the groove at S, at an angle μ. When μ is of such a value that the magnitude of 2δ is increased by, say, $\lambda/2$ at points E and E' for which δ was previously a small fraction of a wavelength, then that part of the vector diagram representing the groove between E and E' approximates to a circle, and the resultant for the whole wavelength of modulation is small (Figure 24b).

The greater the wavelength of the modulation, then, the smaller is the value of μ which effects a given diminution of intensity, and the sharper is the edge observed to the pattern.

This is in fact observed, for while the low frequency patterns on the focal plane are sharply defined, those for higher frequencies are diffuse at the edges, as they are when the surface of the disk is viewed. The edge of the pattern on the focal plane at low frequencies is thus in the position Pϕ, which is what would be expected from considerations of geometrical optics.

11. Extension of Basic Formulae to Focal Plane Patterns

Figure 25 shows, in plan, the formation of a far side pattern of half-width b_f, as in Figure 3(a). The 'focal plane' is at a distance "p" in front of the disk, determined by the usual formula for a spherical mirror, which also holds for a normal plane of a cylindrical mirror, and which gives in this case

$$\frac{1}{p} + \frac{1}{d_2} = \frac{2 \cos \theta}{R} \quad \ldots\ldots\ldots\ldots(4)$$

The intersection of this plane and the limiting ray from the pattern on the disk defines the edge of the focal plane pattern, all other rays from points of maximum modulation slope also passing through this point on the plane.

The half-width of this pattern, b_f', is given by

$$b_f' = b_f - \frac{p}{d_1}(b_f + a_1)$$

$$\therefore b_f = \frac{b_f'}{\left(1 - \frac{p}{d_1}\right)} + \frac{a_1 p}{d - p} \quad \ldots\ldots\ldots\ldots(5)$$

If, in the measurement of b_f', no allowance is made for the effect of the displacement p on the factor converting scale readings to pattern width, then the value found will be in error. The value found, b_f'', will be related to the actual value b_f' by the equation

$$b_f'' = \frac{b_f'}{\left(1 - \frac{p}{d'}\right)}$$

where d' is the distance from the disk to the reflecting face of prism P_4, about which the moving image pivots. If b_f'' is substituted for

$$\frac{b_f'}{\left(1 - \frac{p}{d_1}\right)}$$

in Equation (5) then an error of less than 0.5% will be caused by the inequality of d_1 and d', so that to this accuracy

$$b_f = b_f'' + \frac{a_1 p}{d-p} \quad \ldots\ldots\ldots 6(a)$$

A similar calculation for near-side measurements gives

$$b_n = b_n'' + \frac{a_1 p}{d+p} \quad \ldots\ldots\ldots 6(b)$$

where p is now the distance of the focal plane behind the disk given by

$$\frac{1}{p} - \frac{1}{d_2} = \frac{2 \cos \theta}{R}$$

12. The Resolving Power of the Measuring System

When a telescope is focussed on an infinitesimal luminous source, the image always has a finite extent, however good the lens system. This fundamental limitation of the definition attainable is a diffraction phenomenon, and a formula is derived below enabling the minimum image width to be calculated in terms of the telescope aperture, the distance of the luminous point from the aperture, and the wavelength of light.

Consider a telescope, the aperture of which is defined by a vertical slit of width 2a, and which is focussed upon a plane at a distance d from the slit (Figure 26). Two points on this plane, P_1 and P_2, are spaced at a small horizontal distance h/2 to either side of the axis. In order to determine the apparent width of P_1, it is required to find the variation with h of the spurious illumination observed at P_2 as a result of the light emitted from P_1. This is done in a manner similar to that employed in paragraph 8 i.e. by vector summation along an arc R_2, centred on P_2, of the disturbancesfrom P_1, which are in phase along an arc R_2, centred on P_2. It is again required to determine the variation across the aperture of the distance δ separating the two arcs, and hence the shape of the vector diagram.

The two arcs, each of radius d, touch the plane of the aperture at distances h/2 to either side of the axis, so that the separation q_1 of R_1 from the plane of the aperture is, at any distance e from the axis, a function of (e - h/2), and that of q_2, a function of (e + h/2). The actual expression for q_1 and q_2 can be shown to be

$$q_1 = \frac{(e - h/2)^2}{2d} \text{ and } q_2 = \frac{(e + h/2)^2}{2d}$$

$$\text{But } \delta = q_2 - q_1 = \frac{(e + h/2)^2}{2d} - \frac{(e - h/2)^2}{2d}$$

$$\therefore \delta = \frac{h\,e}{d} \qquad \ldots\ldots\ldots\ldots\ldots\ldots(7)$$

The value, δ_{max}, which δ assumes at the edge of the aperture where $e = a$ is given by

$$\delta_{max} = \pm \frac{ha}{d} \qquad \ldots\ldots\ldots\ldots\ldots\ldots(8)$$

For any value of h the quantity δ is proportional to e, and the vector diagram is in the form of a circle, since equal increments along its length correspond to equal increments of δ, and hence of the phase angle $\frac{2\pi\delta}{\lambda}$.

If h is now varied, the constant length of the vector diagram, corresponding to the length 2a of the arc R_2, will assume a curvature dependent upon the value of δ_{max}, which is proportional to h. Thus for values of h such that the magnitudes of δ_{max} are $\lambda/4$, $\lambda/2$, $\frac{3}{4}\lambda$ and λ respectively, the vector diagram has the form shown in Figure 27.

The variation of intensity of h, due to the curling up of the vector diagram as h increases, is of the form shown in Figure 28, and as this represents the intensity observed at a distance h from the point P_1, the main image of P_1 is seen to extend over a finite width $2h_o$, when h_o is the value of h for which $\delta_{max} = \pm \lambda/2$.

If, now, two neighbouring luminous points are considered, it will be seen that when their separation is less than a certain value, their images will overlap to such an extent that a single broad maximum of illumination will be observed, and the existence of two distinct points will no longer be discernable. It is normally assumed that the critical separation of the two luminous points, for their images to be just resolvable, is equal to h_o, so that the two intensity curves overlap to the extent shown in Figure 29, and h_o is thus taken as the resolving power of the system. Substituting $\delta_{max} = \pm \lambda/2$ in Equation (8) therefore:-

$$h_o = \frac{d\lambda}{2a}$$

In the present apparatus d = 48 inches and 2a = 0.25 inches. Taking $\lambda = 2 \times 10^{-5}$ inches, therefore, we have

$$h_o = \frac{48 \times 2 \times 10^{-5}}{0.25} \text{ inches}$$

$$= 0.004 \text{ inches}$$

13. The Final Form of the Measuring Apparatus

13.1 Development of the Investigation

The present investigation into the light pattern method of measuring the level on a laterally-recorded disk was undertaken initially to develop the "edge-to-edge" method of measuring pattern widths. The ease of measurement by this method has been very marked and the increased accuracy and consistency possible has enabled the scope of the original investigation to be broadened considerably, so that the nature of some fundamental inaccuracies in the light pattern method have been ascertained. Part 2 of this Report has been concerned with an analysis of certain optical interferance and diffraction effects and shows that inaccuracies must occur when the surface of the disk is observed. This information has led to a modification of the measurement itself which is now made with the telescope focussed on the so called "focal plane" instead of the disk surface.

With this acquired background of knowledge it is possible to make a more direct approach to the light pattern measurement embodying the principle of edge-to-edge measurement of the light pattern formed in the focal plane. A direct derivation of the expression for the width of the pattern formed in the focal plane will be given below and it will be shown that a much more compact apparatus than that described here is conceivable. These findings will be embodied in a final light-pattern measuring instrument which is being built in the Research Department.

13.2 Direct Derivation of Focal Plane Pattern Width

Figure 30 represents in plan one groove of a disk being viewed on the far side. The edge of the focal plane pattern at P_ϕ is formed by light reflected from elements of maximum modulation slope ϕ with respect to the unmodulated groove. It was pointed out in paragraph 9.2 that the effective turning of the reflecting surface through an

angle ϕ when the groove is modulated turns the reflected ray through an angle 2ϕ.

For an infinitely narrow light source, therefore, the half-pattern width is given by $b_f' = 2\phi p$ where, as before, p is the distance of the focal plane from the groove under consideration. Thus b_f' is the amount by which the slope ϕ causes the image of the light source to be displaced.

Now the half-width of the light source image depends upon the ratio p/d_2 which is the magnification of a concave mirror when it forms an image at distance p from its surface of an object at distance d_2. The half-width of the image of a finite source of width $2a_2$ formed by the unmodulated groove will be $a_2 \cdot \frac{p}{d_2}$. The half-width of the image formed by the modulated groove will, therefore, be

$$b_f' = 2\phi p + a_2 \cdot \frac{p}{d_2}$$

Now $p = \dfrac{R/2 \cos \theta}{1 - R/2 \cos \theta \cdot d_2}$ from Equation 4 of paragraph 11

$$\therefore b_f' = \frac{\phi \, R/\cos \theta}{1 - R/2 \cos \theta \cdot d_2} + \frac{a_2/d_2 \; R/2 \cos \theta}{1 - R/2 \cos \theta \cdot d_2}$$

$$\text{and } \phi \frac{R}{\cos \theta} = b_f' \left[1 - \frac{R}{2 \cos \theta} \left(\frac{1}{d_2} \right) \right] - \frac{R}{2 \cos \theta} \left(\frac{a_2}{d_2} \right)$$

but $\phi \cdot \dfrac{R}{\cos \theta} = b$ from Equation 2(a) paragraph 1.

$$\therefore b = b_f' \left[1 - \frac{R}{2 \cos \theta} \left(\frac{1}{d_2} \right) \right] - \frac{R}{2 \cos \theta} \left(\frac{a_2}{d_2} \right) \quad \ldots (9)$$

Equation (9) does not contain terms in d_1 or a_1. This indicates that the only stipulation which need be made about the viewing system is that its depth of focus shall be sufficient to allow the focal plane to be observed without vertical de-focussing causing the different patterns to overlap. It also follows that if a collimator source is used (when d_2 is effectively infinite) the formula becomes

$$b = b_f' - \frac{R}{2 \cos \theta} \left(\frac{a_2}{f} \right)$$

where f is the focal length of the collimator, since the source at infinity will have an angular spread of $\frac{a_2}{f}$. Thus by using a long focus collimator and a very narrow light source it should be possible to make the "no-mod" term negligibly small and the measuring system direct reading for all but very low levels. Clearly, all these conditions, with the depth of focus proviso outline above, indicate that a much smaller apparatus can be made.

When the light source is at infinity $p \rightarrow R/2 \cos\theta$. If $\theta = 45^\circ$, $\cos\theta = \frac{1}{\sqrt{2}}$ so that $p = \frac{R}{2 \cos 45^\circ} = R \cos 45^\circ$.

But $R \cos 45^\circ$ is the horizontal distance from the groove under consideration to the centre of the disk. Thus when the light source is at infinity the focal plane for any radius of the disk coincides with the vertical plane through the centre of the disk. The existing trolley system, by which the disk is moved in both vertical and horizontal directions, may then be replaced by a vertical lift since the focal plane will always be the same distance from the telescope and the prism system. One focussing will then cover the whole disk (near and far side) and the magnification of prism-rotation/image displacement relationship (paragraph 11) will be the same for the entire disk.

13.3 Alternative Derivation of Focal Plane Pattern Width

Equation 5 of paragraph 11 gives the hypothetical half-pattern width b_f on the disk in terms of the half-width b_f' measured on the focal plane as

$$b_f = \frac{b_f'}{\left(1 - \frac{p}{d_1}\right)} + \frac{a_1 p}{d - p}$$

where p is the distance of the focal plane from the disk. Equation 1(a) of paragraph 1 gives the half-width b of the pattern viewed under ideal conditions, in terms of the quantity b_f, as

$$b = b_f \left[1 - \frac{R}{2 \cos\theta}\left(\frac{1}{d_1} + \frac{1}{d_2}\right)\right] - \frac{R}{2 \cos\theta}\left(\frac{a_1}{d_1} + \frac{a_2}{d_2}\right)$$

Substituting Equation 5 into 1(a) then gives

$$b = b_f' \left[1 - \frac{R}{2 \cos\theta}\left(\frac{1}{d_2}\right)\right] - \frac{R}{2 \cos\theta}\left(\frac{a_2}{d_2}\right)$$ which is the

result obtained by the direct analysis. It is to be expected that the combination of Equations 1(a) and 5 would give a result which is independent of the viewing aperture a_1 and the viewing distance d_1 since the focal plane pattern is of definite extent irrespective of the manner in which it is viewed.

In the present apparatus it is still necessary to know d_1 since it is convenient to express the focal-plane widths measured in terms of a calibration made by laying a graduated scale upon the disk surface (paragraph 11) but the quantity a_1 need not actually be known.

MJB

ISSUE
1
23-8-50

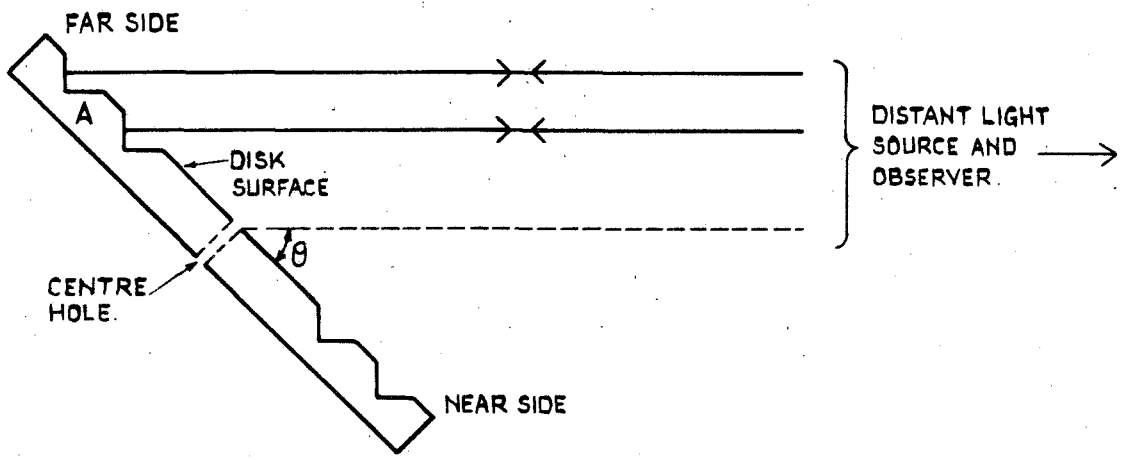

FIG 1

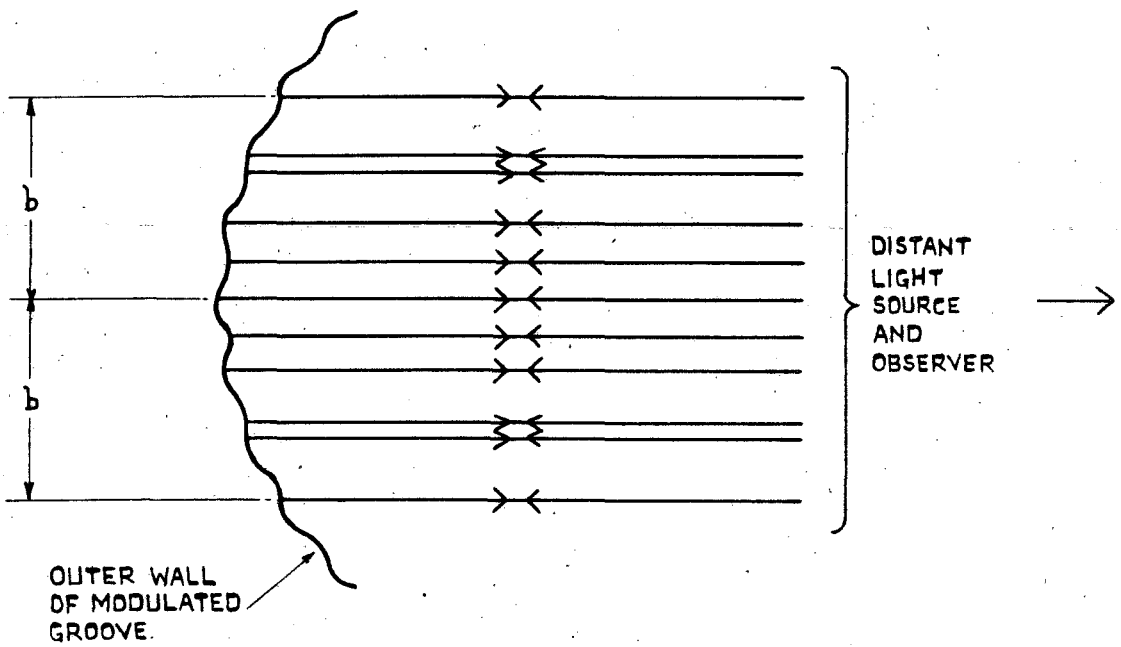

FIG 2

BBC

DS/1/OC

A RECONSIDERATION OF LIGHT PATTERN MEASUREMENTS IN LATERAL DISK RECORDING.

RESEARCH DEPT.

DR'N	W.H.
CH'D	W.K.E.B.
AP'D	P.B.C.

REPORT
C.077
17 SHEETS No 1

ISSUE
1
23-8-50

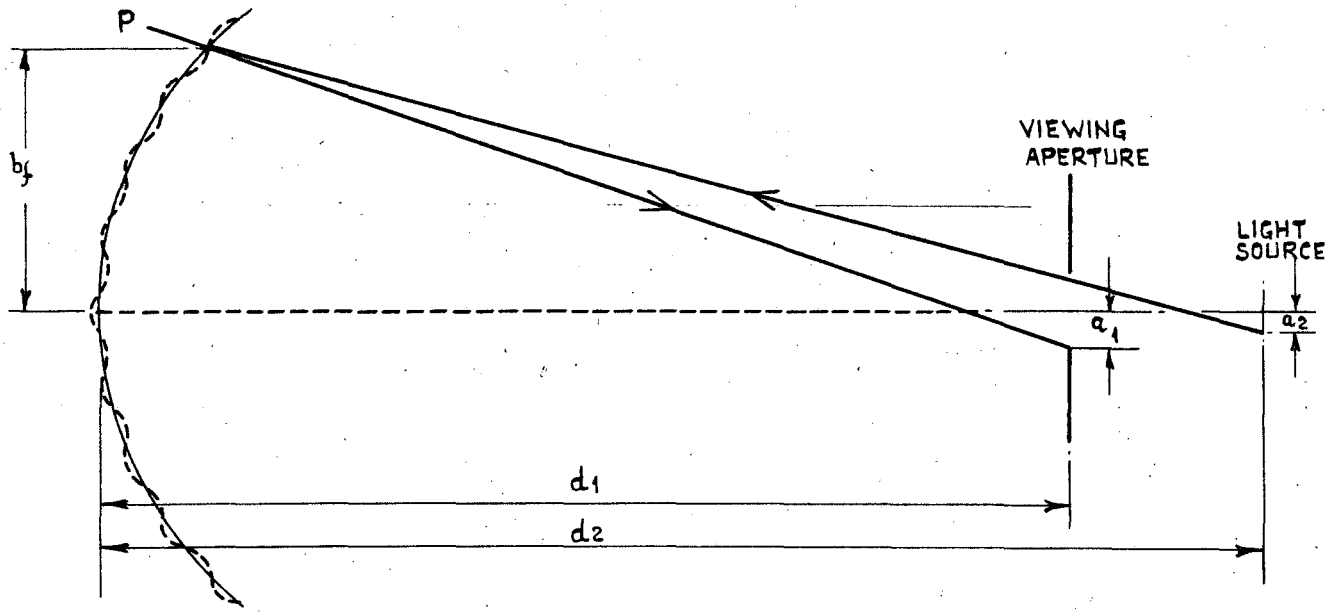

FIG 3a

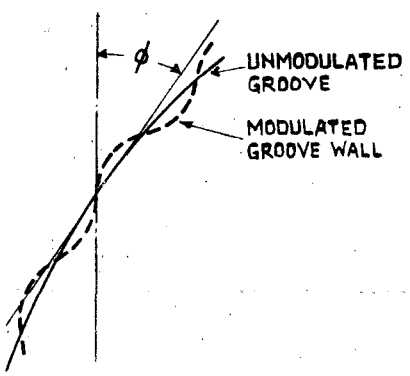

FIG 3b

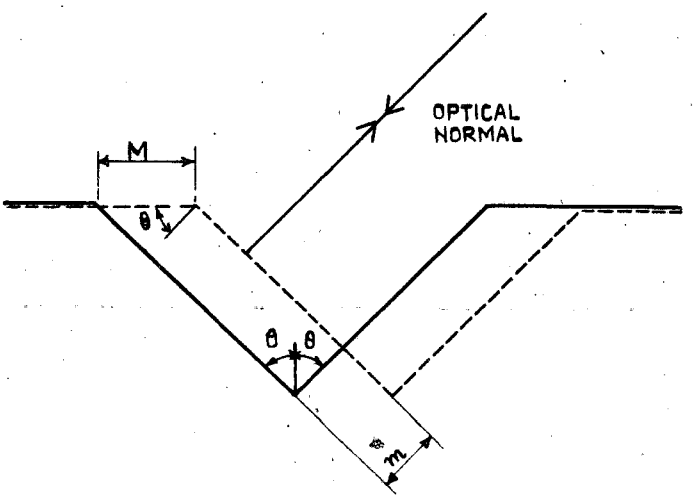

FIG 4

BBC

DS/1/OC

A RECONSIDERATION OF LIGHT PATTERN MEASUREMENTS IN LATERAL DISK RECORDING.

RESEARCH DEPT.

DR'N	W.H.	REPORT
CH'D	W.K.S.	C.077
AP'D	P.G.G.	17 SHEETS No 2

ISSUE

23-8-50

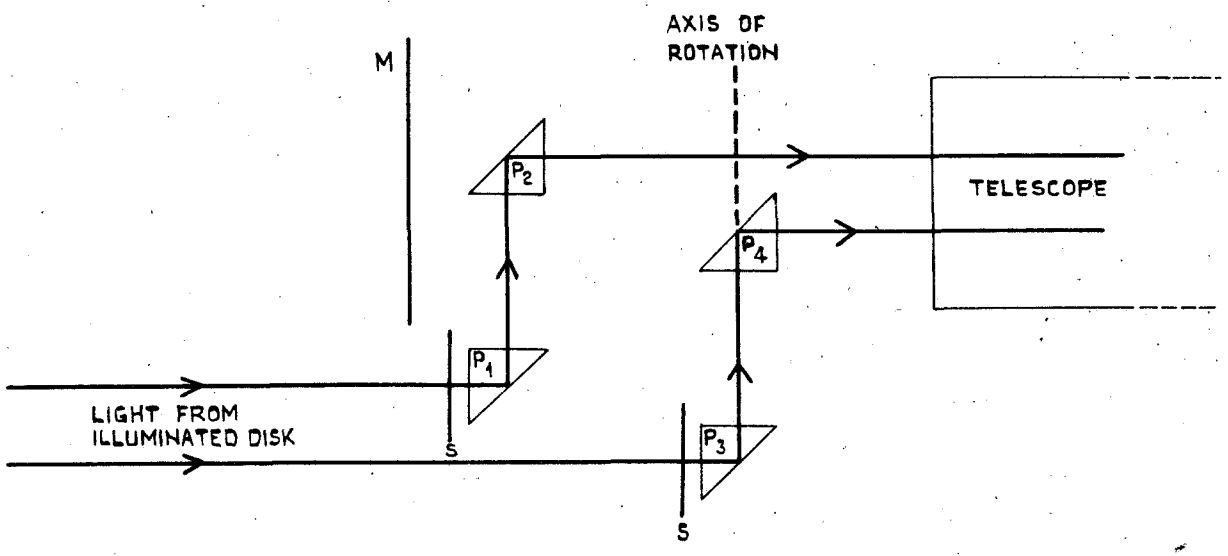

FIG 5

BBC

DS/1/OC

A RECONSIDERATION OF LIGHT PATTERN MEASUREMENTS IN LATERAL DISK RECORDING.

RESEARCH DEPT.

DR'N	W.H.
CH'D	M.K.E.P.
AP'D	P.G.

REPORT C.077

17 SHEETS No 3

ISSUE
1
23-8-50

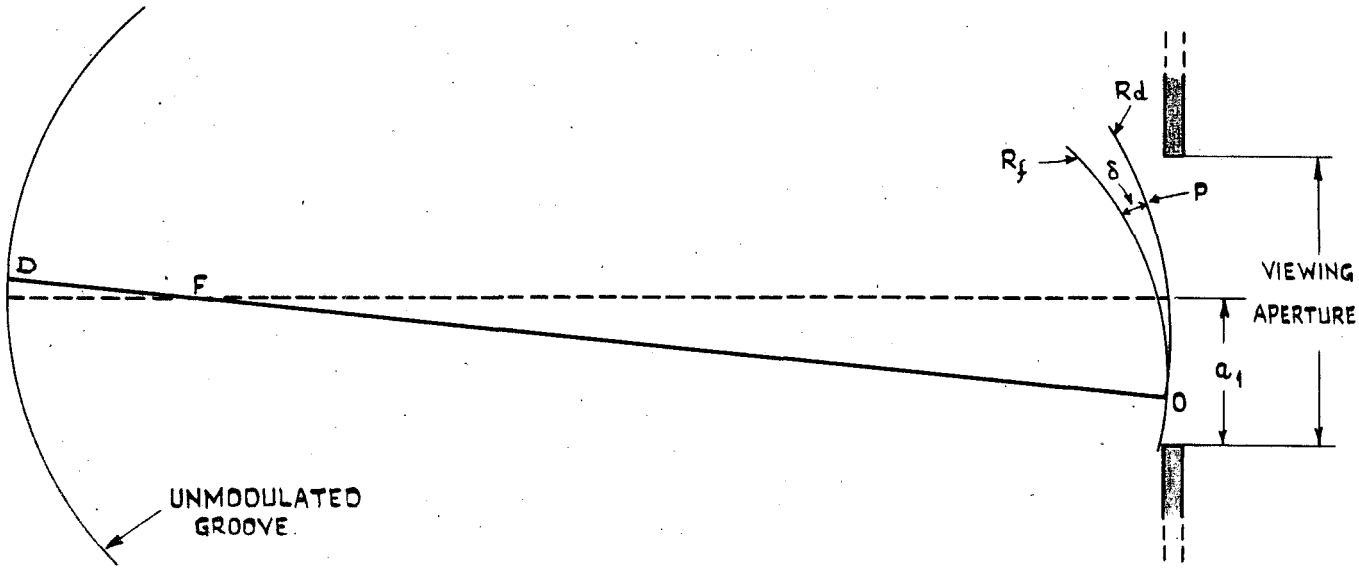

FIG 6

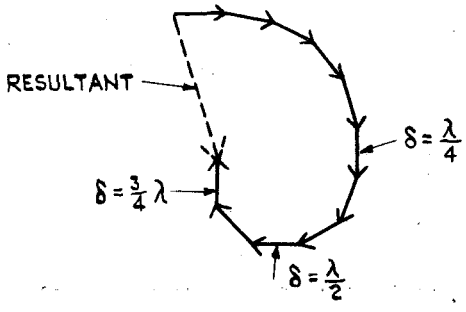

FIG 7a

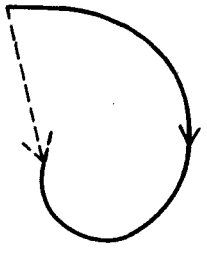

FIG 7b

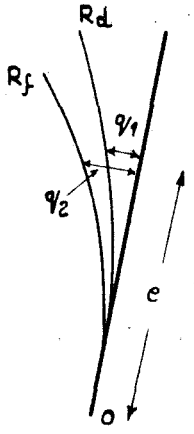

FIG 8

BBC

DS/1/OC

A RECONSIDERATION OF LIGHT PATTERN MEASUREMENTS IN LATERAL DISK RECORDING.

RESEARCH DEPT.

DR'N	W.H.	REPORT
CH'D	[illegible]	C.077
AP'D	P.E.C.	17 SHEETS No 4

ISSUE
1
23-8-50

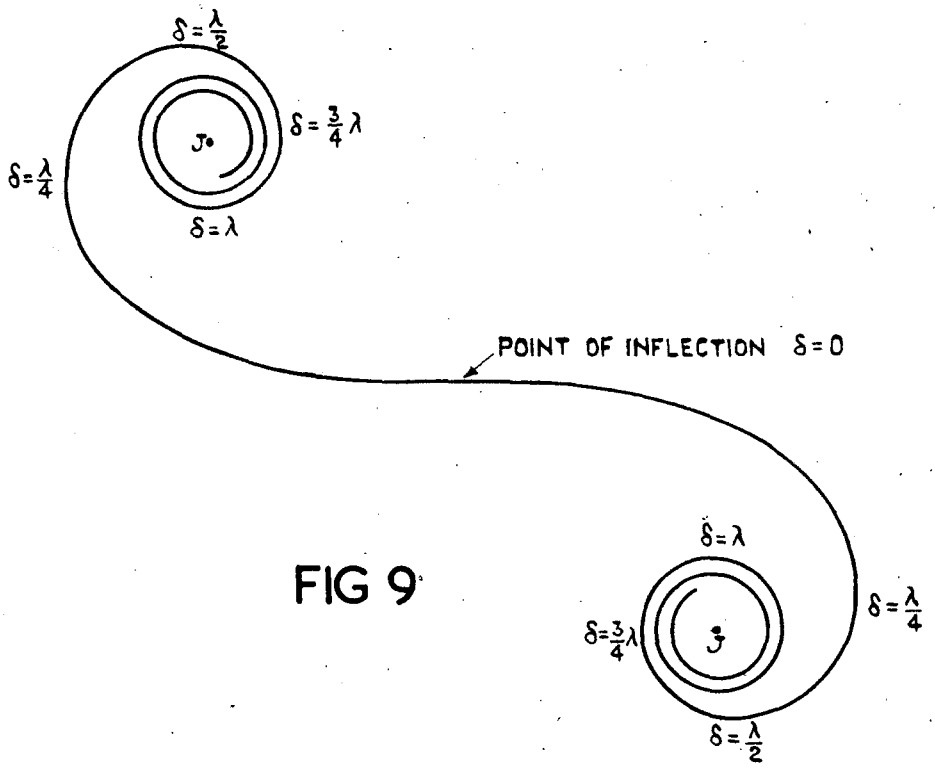

FIG 9

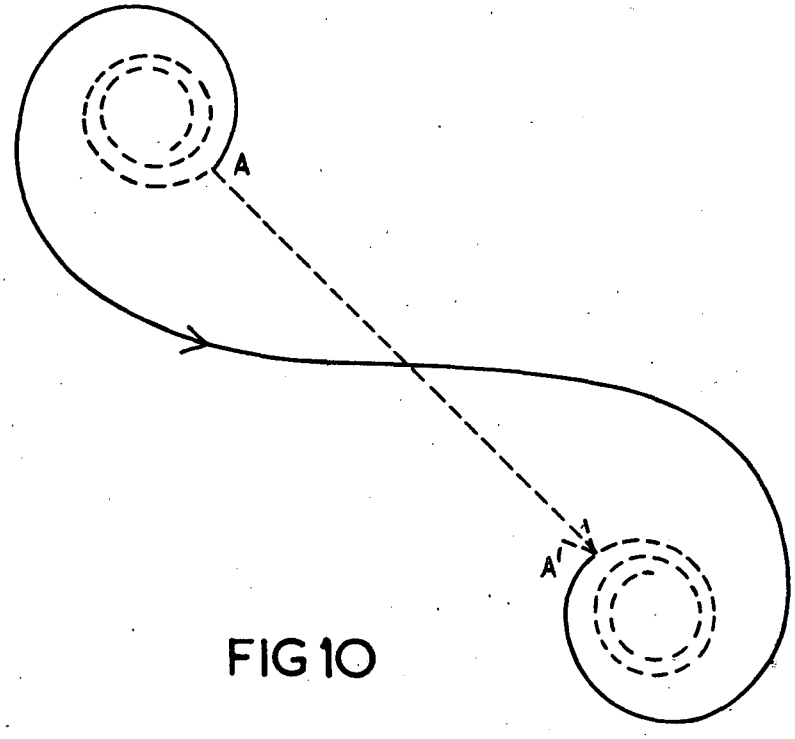

FIG 10

BBC

DS/1/OC

A RECONSIDERATION OF LIGHT PATTERN MEASUREMENTS IN LATERAL DISK RECORDING.

RESEARCH DEPT.

DR'N	W.H.
CH'D	
AP'D	

REPORT C.077

17 SHEETS No.5

ISSUE
1
23-8-50

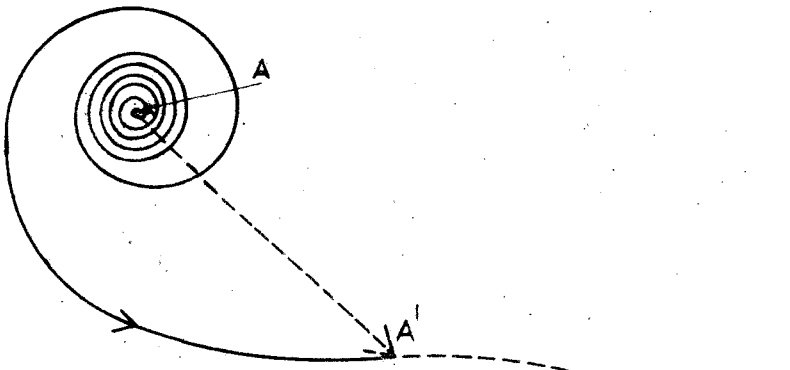

FIG 11

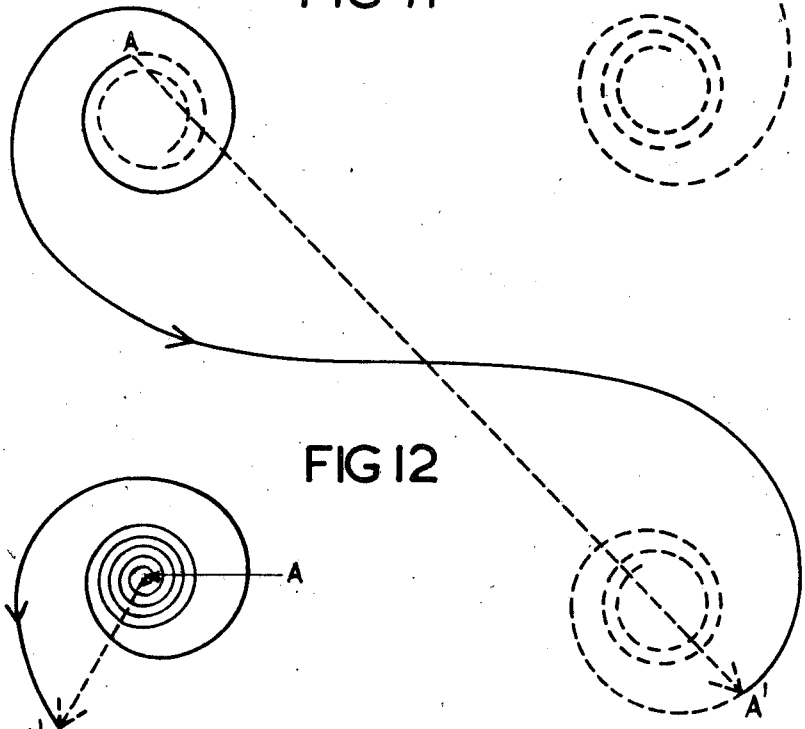

FIG 12

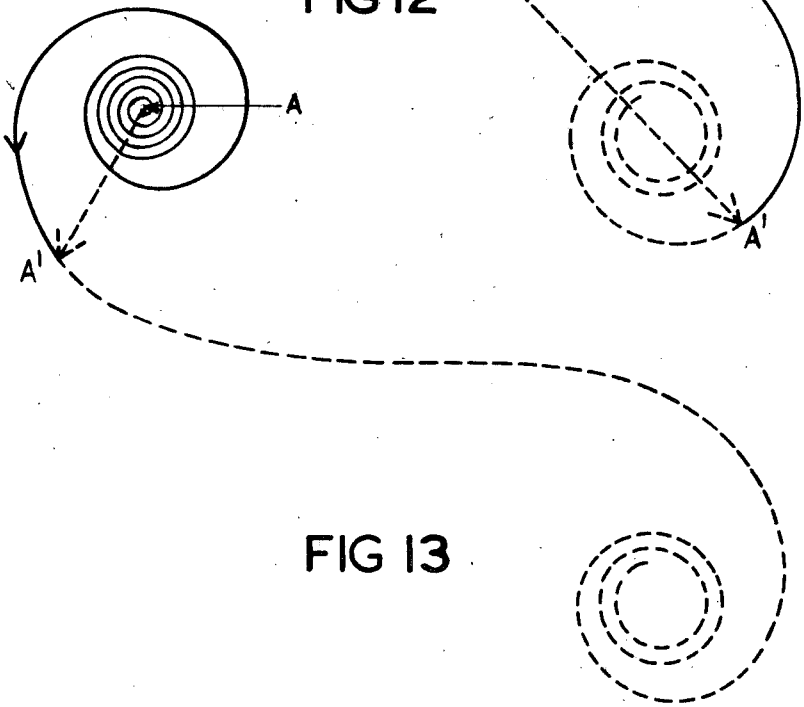

FIG 13

BBC

DS/1/OC

A RECONSIDERATION OF LIGHT PATTERN MEASUREMENTS IN LATERAL DISK RECORDING.

RESEARCH DEPT.

DR'N	W.H.
CH'D	W.K.C.S.
AP'D	P.L.C.

REPORT
C.077
17 SHEETS No 6

ISSUE
1
23-8-50

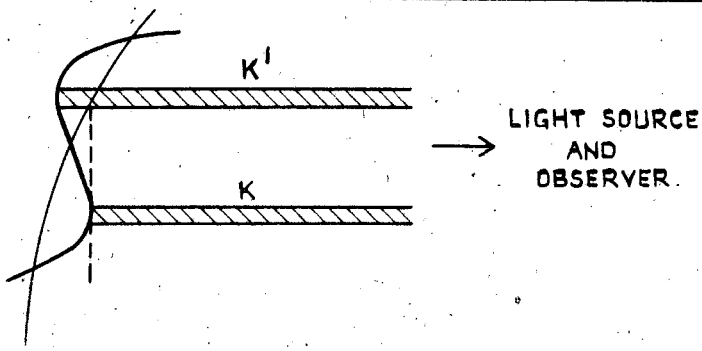

FIG 14

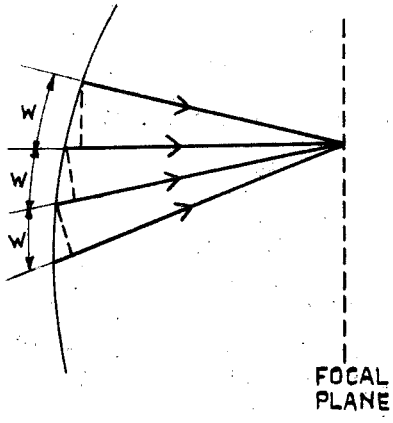

FIG 15

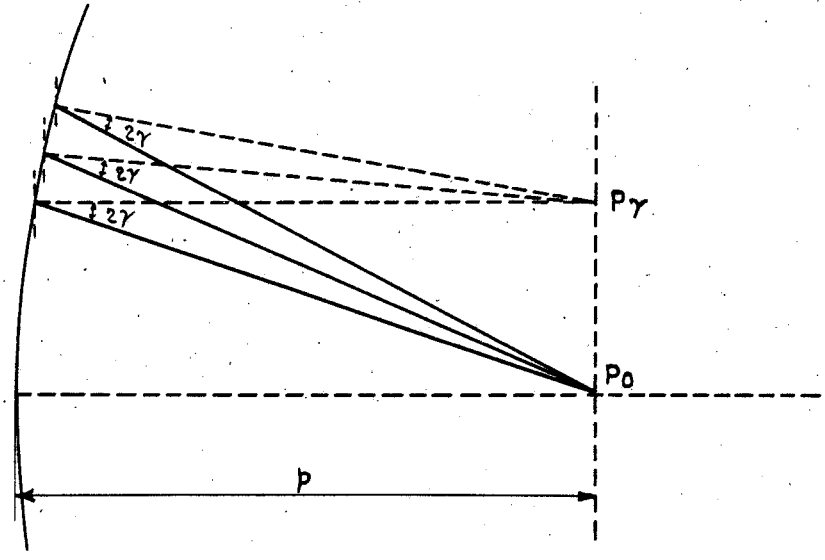

FIG 16

BBC

DS/1/OC

A RECONSIDERATION OF LIGHT PATTERN MEASUREMENTS IN LATERAL DISK RECORDING.

RESEARCH DEPT.

DR'N	W.H.	REPORT
CH'D	W.K.E.B.	C.077
AP'D	P.L.C.	17 SHEETS No 7

ISSUE
1
23-8-50

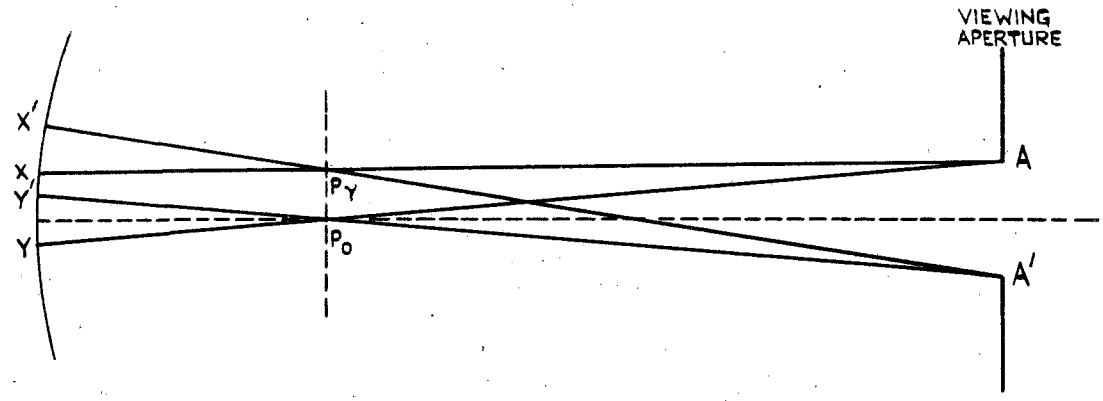

FIG 17

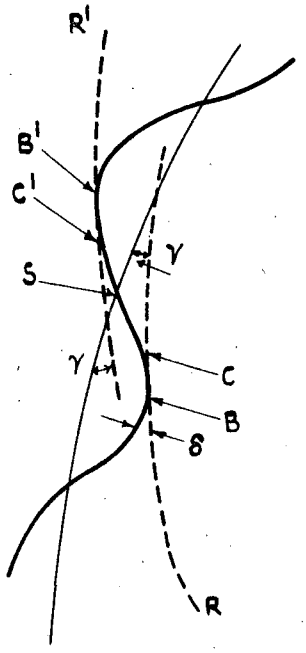

FIG 18

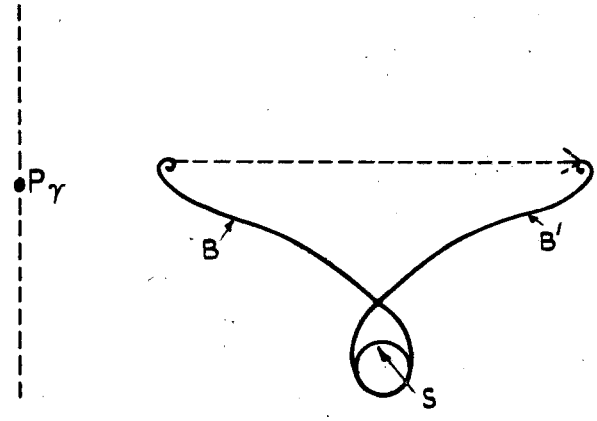

FIG 19

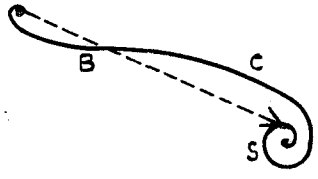

FIG 20a

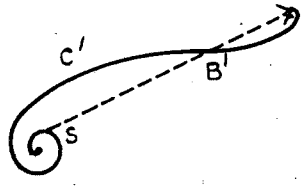

FIG 20b

BBC

DS/1/OC

A RECONSIDERATION OF LIGHT PATTERN MEASUREMENTS IN LATERAL DISK RECORDING.

RESEARCH DEPT.

DR'N	W.H.
CH'D	W.K.F.C.
AP'D	P.P.C.

REPORT
C.077
17 SHEETS No 8

ISSUE
1
23-8-50

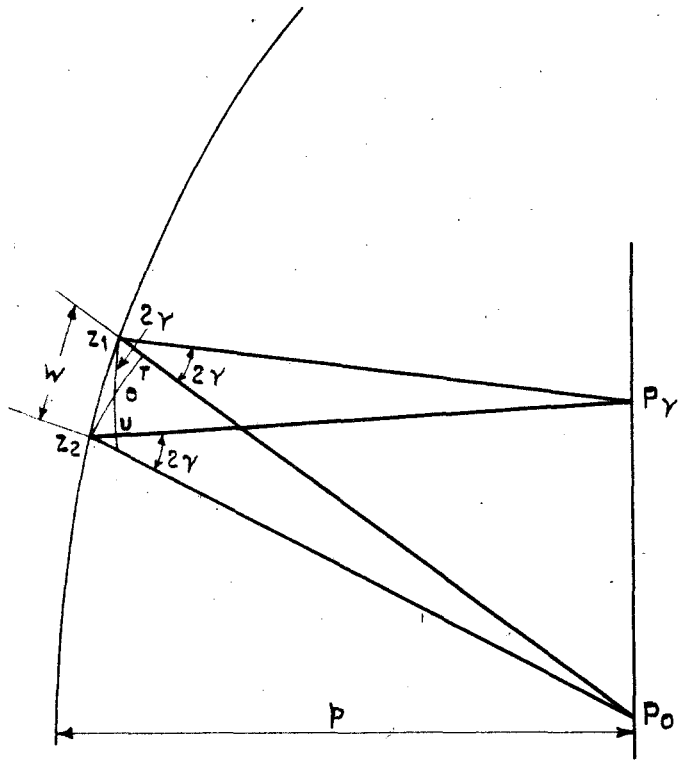

FIG 21

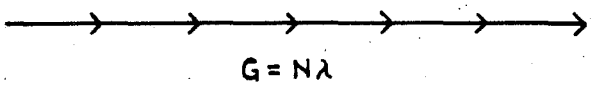

$G = N\lambda$

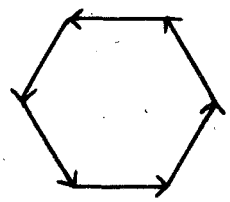

$G = \left(N + \frac{1}{6}\right)\lambda$

FIG 22

BBC

DS/1/OC

A RECONSIDERATION OF LIGHT PATTERN MEASUREMENTS IN LATERAL DISK RECORDING.

RESEARCH DEPT.

DR'N	W.H.
CH'D	W.J.G.B.
AP'D	P.L.A.

REPORT
C.077
17 SHEETS No 9

ISSUE
1
23-8-50

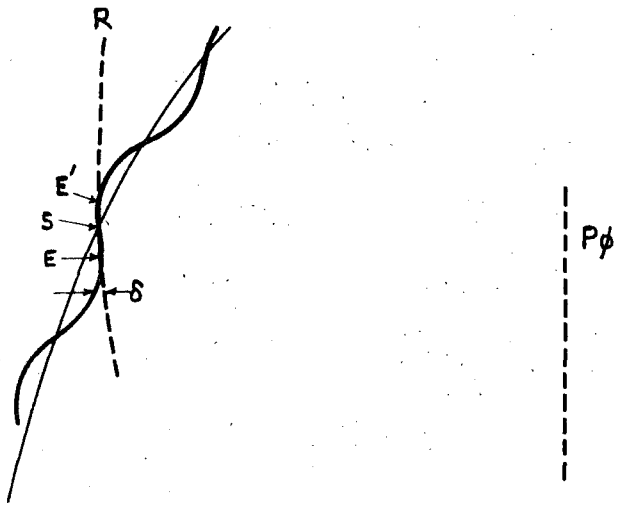

FIG 23

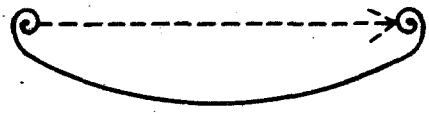

FIG 24a

FIG 24b

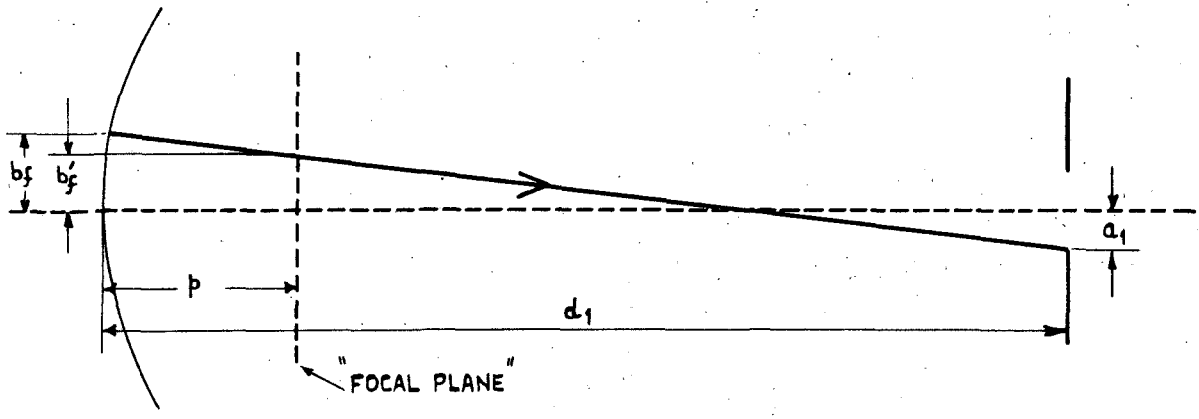

FIG 25

BBC

DS/1/OC

A RECONSIDERATION OF LIGHT PATTERN MEASUREMENTS IN LATERAL DISK RECORDING.

RESEARCH DEPT.

DR'N	W.H.
CH'D	W.R.E.G.
AP'D	P.L.A.

REPORT
C.077
17 SHEETS No.10

ISSUE
1
23-8-50

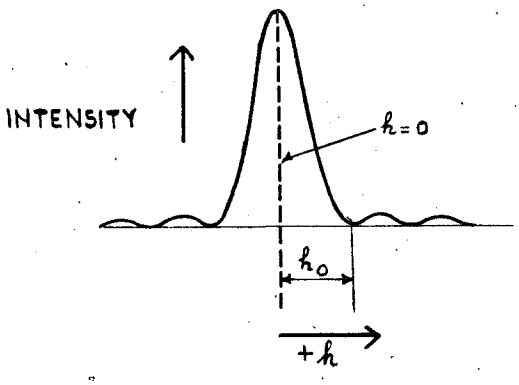

FIG 28

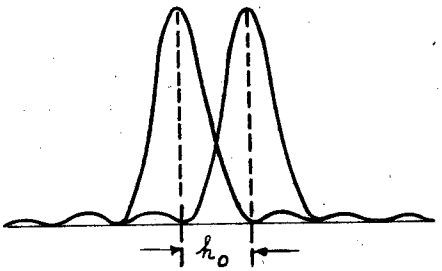

FIG 29

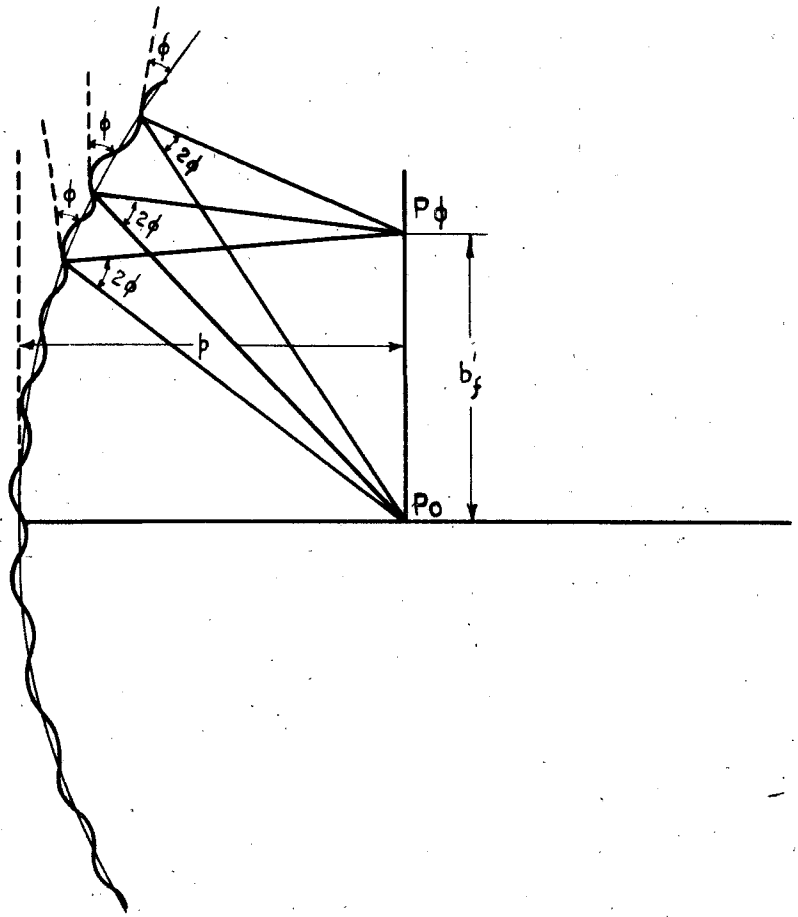

FIG 30

BBC

DS/1/OC

A RECONSIDERATION OF LIGHT PATTERN MEASUREMENTS IN LATERAL DISK RECORDING.

RESEARCH DEPT.
DR'N W.H.
CH'D W.K.E.G.
AP'D P.L.H.
REPORT
C.077
17 SHEETS No 12

ISSUE
1
23-8-50

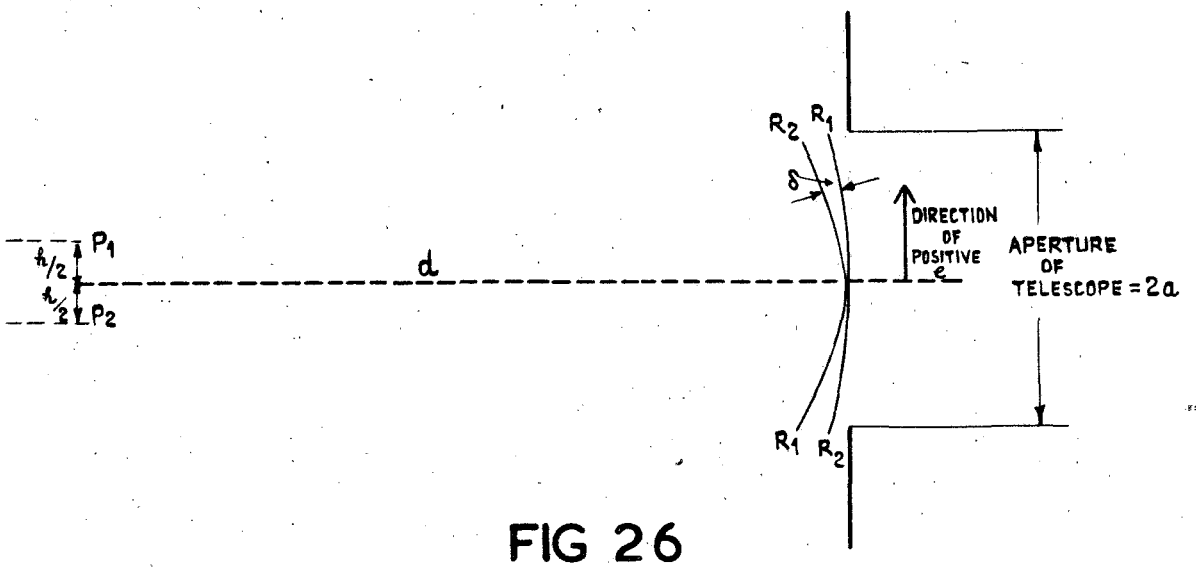

FIG 26

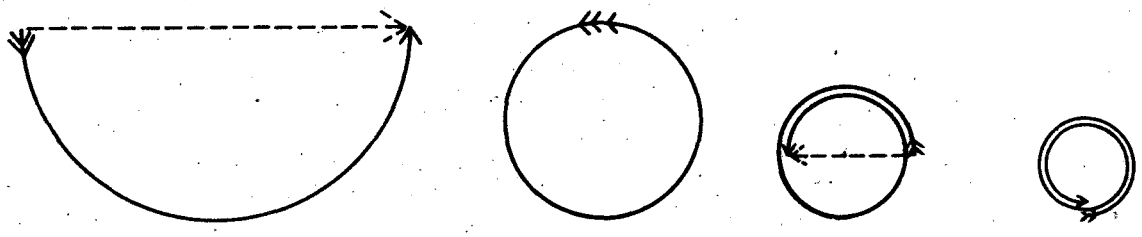

FIG 27

BBC

DS/1/OC

A RECONSIDERATION OF LIGHT PATTERN MEASUREMENTS IN LATERAL DISK RECORDING.

RESEARCH DEPT

DR'N	W.H.
CH'D	W.K.S.C.
AP'D	P.F.D.

REPORT C.077

17 SHEETS No.11

ISSUE
1
23-8-50

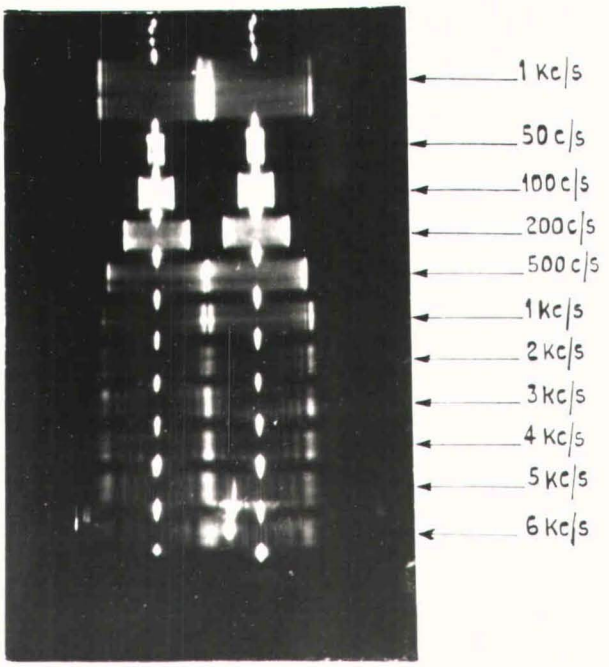

PLATE I

DOUBLE PATTERN DISPLAY WITH
EDGE TO EDGE COINCIDENCE
AT 500 CYCLES.

BBC

DS/1/OB

A RECONSIDERATION OF LIGHT PATTERN MEASUREMENTS IN LATERAL DISK RECORDING.

RESEARCH DEPT

DR'N	W.H.
CH'D	K.E.G.
AP'D	

REPORT
C.077
17 SHEETS No.13

ISSUE
1
23-8-50

PLATE II
GENERAL VIEW OF APPARATUS

BBC

DS/1/OB

A RECONSIDERATION OF LIGHT PATTERN MEASUREMENTS IN LATERAL DISK RECORDING.

RESEARCH DEPT

DR'N	W.H.
CH'D	W.K.S.L.
AP'D	P.C.D.

REPORT
C.077
17 SHEETS No 14

ISSUE
1
23-8-50

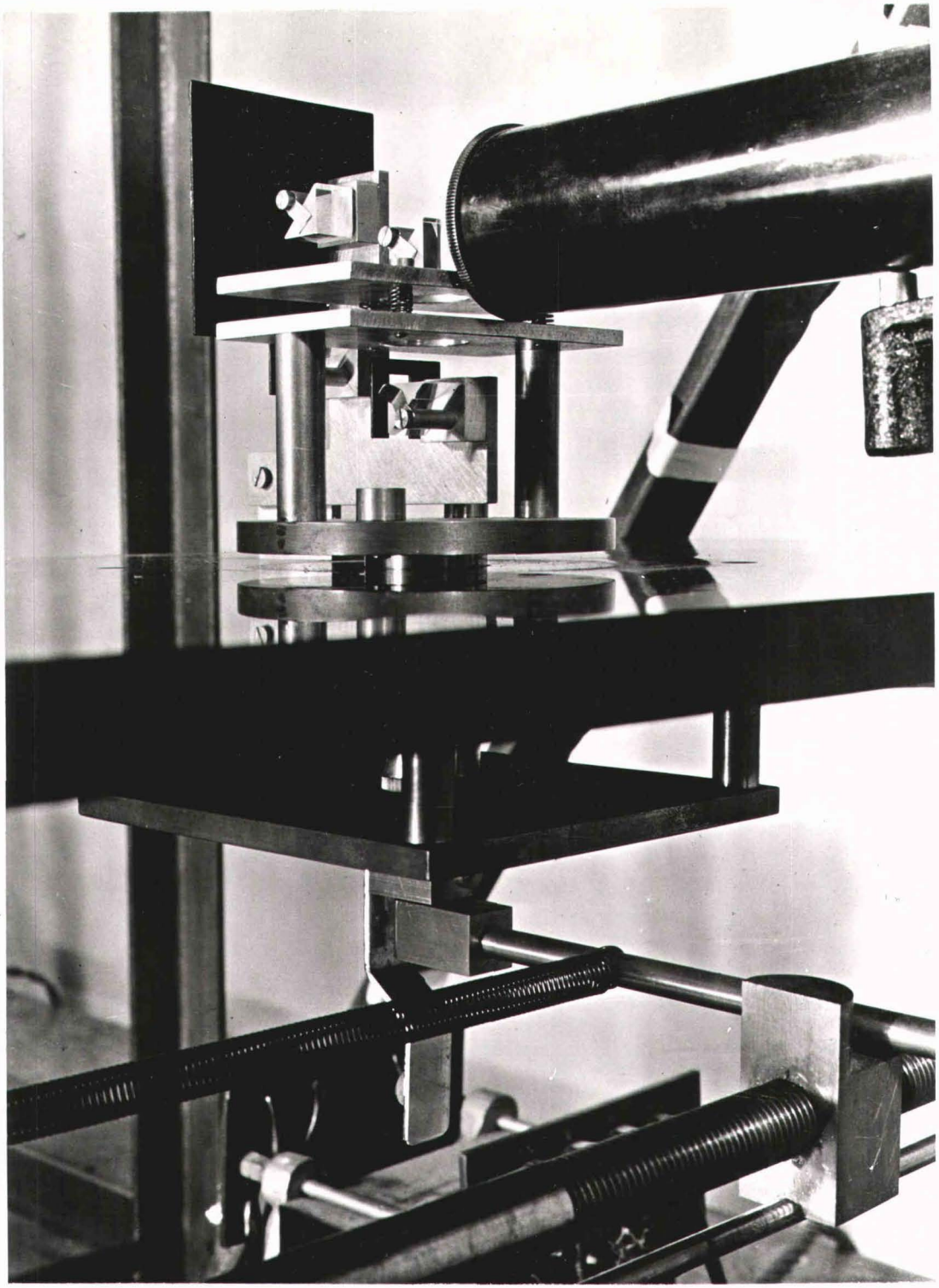

PLATE III

PRISM SYSTEM & ROTATIONAL ASSEMBLY.

BBC

DS/1/OB

A RECONSIDERATION OF LIGHT PATTERN MEASUREMENTS IN LATERAL DISK RECORDING.

RESEARCH DEPT

DR'N	W.H.	REPORT
CH'D	W.K.E.G.	C.077
AP'D	P.B.L.	17 SHEETS No 15

ISSUE
1
23-8-50

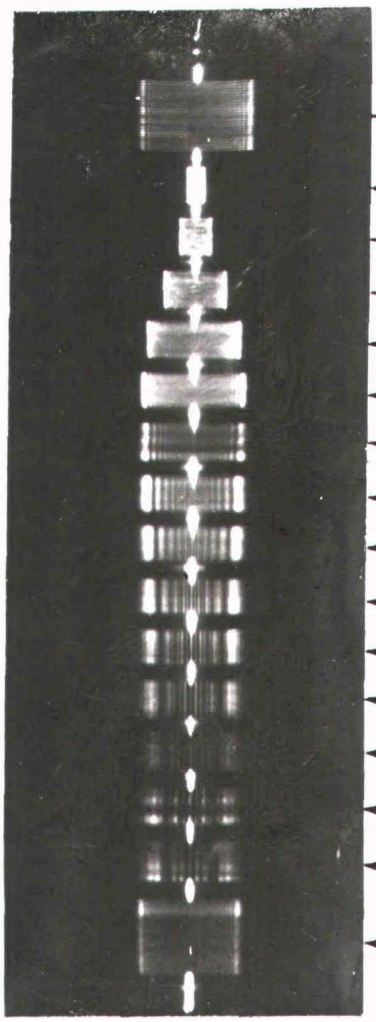

PLATE IV

APPEARANCE OF BLACK LINE IN THE "NO-MOD" BAND.

PLATE V

LIGHT PATTERN SHOWING INTERFERENCE FRINGES.

BBC

DS/1/OB

A RECONSIDERATION OF LIGHT PATTERN MEASUREMENTS IN LATERAL DISK RECORDING.

RESEARCH DEPT

DR'N	W.H.	REPORT
CH'D	J.W.C.S.	C.077
AP'D	—	17 SHEETS No 16

ISSUE
1
23-8-50

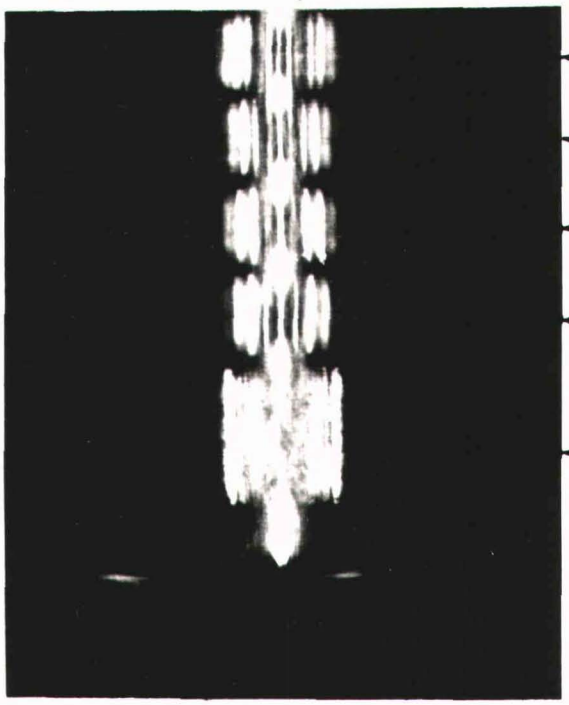

PLATE VI

LIGHT PATTERN SHOWING
'm' AND 'W' FRINGES SEPARATED.

BBC

DS/1/OB

A RECONSIDERATION OF LIGHT PATTERN MEASUREMENTS IN LATERAL DISK RECORDING.

RESEARCH DEPT

DR'N	W.H.	REPORT
CH'D	W.K.E.S	C.077
AP'D		17 SHEETS No. 17